The Concept of Diagonal Approximated Signature: New Surrogate Modeling Approach for Continuous-State Systems in the Context of Resilience Optimization

Niklas R. Winnewisser*,[1], Julian Salomon[1], Matteo Broggi[1] and Michael Beer[1,2,3]

[1]*Institute for Risk and Reliability, Leibniz University Hanover, Hanover 30167, Germany.*
[2]*Institute for Risk and Uncertainty, University of Liverpool, Liverpool L69 7ZF, United Kingdom.*
[3]*International Joint Research Center for Resilient Infrastructure & International Joint Research Center for Engineering Reliability and Stochastic Mechanics, Tongji University, Shanghai 200070, China.*

Abstract

The increasing size and complexity of modern systems presents engineers with the inevitable challenge of developing more efficient yet comprehensive computational tools that enable sound analyses and ensure stable system operation. The previously introduced resilience framework for complex and sub-structured systems provides a solid foundation for comprehensive stakeholder decision-making, taking into account limited resources. In their work, a survival function approach based on the concept of survival signature models the reliability of system components and subsystems. However, it is limited to a binary component and system state consideration. This limitation needs to be overcome to ensure comprehensive resilience analyses of real world systems. An extension is needed that guarantees both maintaining the existing advantages of the original resilience framework, yet enables continuous performance consideration.

This work introduces the continuous-state survival function and concept of the Diagonal Approximated Signature (DAS) as a corresponding surrogate model. The proposed concept is based on combinatorial decomposition adapted from the concept of survival signature. This allows for the advantageous property of separating topological and probabilistic information. Potentially high-dimensional coherent structure functions are the foundation. A stochastic process models the time-dependent degradation of the continuous-state components. The proposed approach enables direct computation of the continuous-state survival function by means of an explicit formula and a stored DAS, avoiding costly online Monte Carlos Simulation (MCS) and overcoming the limitation of a binary component and system state consideration during resilience optimization for sub-structured systems. A proof of concept is provided for multi-dimensional systems and an arbitrary infrastructure system.

Keywords: Surrogate Modeling, Continuous-State System, Survival Function, Coherent Structure Function, Resilience Optimization, System Reliability, Monte Carlo Simulation

*winnewisser@irz.uni-hannover.de, published in 2023

1 Introduction

Engineering systems, such as infrastructure networks and complex machines, are ubiquitous worldwide and form the backbone of modern societies. As societies grow, these systems become increasingly sophisticated in size and complexity. Evidently, the stable operation of such systems is crucial for the economy and an undisturbed and safe everyday life of civilians. This challenge is exacerbated by exposure to an increasingly inhospitable, changing and uncertain environment. It is evident that it is exceedingly difficult if not impossible to identify and prevent all potential adverse impacts. The focus in design and maintenance of complex systems has to

be extended from a pure failure prevention and failure persistence strategy to the capabilities of adaptation and recovery. The concept of resilience meets exactly these needs both from a technical and economic point of view and ensures steady functioning [1, 2, 3]. Consequently, there is an increasing need for sophisticated and efficient computational tools that adapt this perspective in order to exploit the potential emerging benefits in engineering practice.

A fundamental precondition for the assessment of resilience of complex systems is an appropriate quantitative resilience metric. In [4, 5, 6], the authors present a broad review of current resilience metrics. In [7], Linkov and Trump provided a critical analysis of resilience definitions and metrics found in literature, their practical application and specifically compare them to the concept of the traditional notion of risk. Hosseini et al. presented in [5] a categorization scheme for resilience quantification approaches. Among these, performance-based resilience metrics are the most common and are based on comparing the performance of a system before and after an adverse event. Theoretically, such an adverse event could correspond to rare shock events on a large time scale or persistent degrading effects on an infinitesimally small time scale. Further subcategories distinguish between time in-/dependence and characterization as deterministic or probabilistic. As motivated in [5] and [8], it is assumed that a performance-based and time-dependent metric is capable of considering the following system states before and after a disruptive event:

- The initial state that remains unchanged until the occurrence of an effectively disruptive event, characterized by system reliability, that is interpreted as the ability of the system to sustain typical performance prior to a disruptive event [5, 9].
- The disrupted state, determined by the system robustness, i.e., the ability of the system to mitigate an effectively disruptive event and its counterpart, vulnerability, represented by a potential loss of performance after the occurrence of a disruptive event [10, 11].
- The recoverability of the system characterizes the duration of the degraded state and the recovery to a new stable state [8, 10].

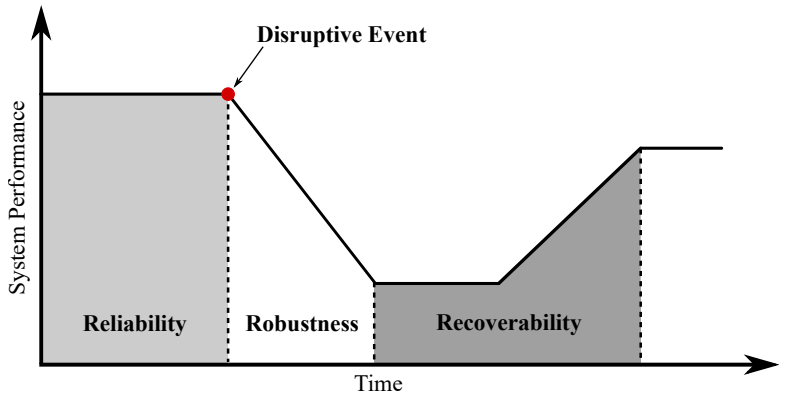

Figure 1: The concept of resilience - three essential phases, adapted from [8].

Figure 1 illustrates these system states and their transitions simplified for a single effectively disruptive event and its potentially infinitesimal small period. Note that the terminologies concerning the governing properties, phases and states presented here, although in their physical interpretation perceived alike or at least similarly, are discussed in literature partly controversially. Thus, for example, what is described here, and, e.g., in [11], as system robustness is referred to as resistance of a system, as in [12]. In fact, the boundaries between the interpretations of reliability and robustness are fluid when extending the conventional perspective as

shall be seen in the further course of this work. For the developments subsequently proposed, it is critical to define a concise interpretation of reliability from a probabilistic perspective. In accordance with [13], let reliability refer to the probability of a system or some entity under consideration to uninterruptedly perform a certain specified function during a stated interval of a life variable, e.g., time, within a certain specified environment.

In the field of engineering, resilience as a concept has consistently gained popularity in recent years [4, 14]. There are numerous ways to improve the resilience of systems. However, there are limits to available resources, and resilience cannot be increased indefinitely. Therefore, it is important not only to be able to differentiate and balance between different resilience-enhancing measures, but also to take into account their monetary aspects [15, 16]. In [17], Salomon et al. present a method for determining the most cost-efficient allocation of resilience-enhancing investments. Further, current research related to resilience focuses on improved metrics for quantifying resilience, such as those proposed in [18], and overarching frameworks for stakeholder decision-making, such as for transportation networks in the presence of seismic hazards [19]. Other recent studies have examined the complexity of real-world infrastructure systems, the consequences of failures, recovery sequences, and various externalities. For instance, in [20], the authors demonstrated the tremendous complexity of modern critical infrastructures and their multifactorial nature as cyber-human-physical systems, and explored appropriate modeling and resilience analysis techniques. Moreover, the studies [21] and [22] address the implications for decision-making considering stakeholder priorities and enhancement or recovery strategies. Climate change challenges have been explored in the context of resilience, e.g., in [23]. A comprehensive literature review of resilience assessment frameworks balancing both resources and performance can be found in [24].

Salomon et al. recently introduced in [25] an efficient resilience framework for large, complex and sub-structured systems, providing a solid foundation for comprehensive stakeholder decision-making, taking into account limited resources. In their work, a survival function approach based on the concept of survival signature, first introduced in [26], models the reliability of system components and subsystems of investigated systems. This reliability approach separates information on the topological (sub)system reliability and the component failure time behavior. Thereby, the survival signature captures the topological information in an efficient manner [27] and thus, can be seen as a type of surrogate modeling technique. This allows for significantly reduced computational effort when it comes to repeated model evaluations, as the demanding evaluation of the topological system model is circumvented [28]. This is all the more relevant the larger and more complex the system under consideration is. The repeated model evaluations are of crucial importance when the parameters examined during the resilience optimization affect the probability structure of the system components. This results in a high number of changes in the probability structure during the resilience analysis, which can be ideally covered by the separation property of the survival signature with minimal computational effort.

A major restriction of the survival signature in its original form is the limitation to a binary component and system state consideration. Consequently, the resilience framework for complex and sub-structured systems in [25] is subject to the same constraints during resilience optimization. However, for a comprehensive resilience analysis of real world systems, a continuous component and system performance state consideration is an indispensable prerequisite. Therefore, an extension is needed that guarantees both the already existing advantages of the resilience framework in [25] based on the original form of the survival signature, yet enables continuous performance consideration.

The most widespread reliability assessment methods follow a binary-state consideration, i.e., reducing the consideration of system performance to the set of the two states of either

perfect functioning or complete failure, compare [29]. Jain et al. states that the "Majority of the existing models have computed system reliability at a holistic level but fail to consider the interactions at component and sub-system levels [...]." In [30], Yang & Xue highlight the importance of a continuous-state consideration in reliability analysis. It is evident that the consideration of continuous component and (sub)system states is equally important for resilience analysis and thus indispensable for realistic resilience optimization. In the last years several researchers proposed various concepts that bring the survival signature to a multi-state consideration, e.g., see [31, 32, 33, 34], which can be seen as a first step in development, towards continuous consideration and potential implementation into proposed resilience framework for sub-structured complex systems [25].

In the current work, theoretical fundamentals are first summarized. Then the concept of the DAS is introduced as a new surrogate modeling approach, based on the concept of survival signature and potentially high-dimensional coherent structure functions describing the relationship between degrading components and corresponding continuous-state system performance. The proposed approach enables direct computation of continuous-state survival function by means of an explicit formula and a stored DAS, thus avoiding a costly online MCS and overcoming the limitation of a binary component and system state consideration. A proof of concept is provided for multi-dimensional systems consisting of min- and max-operators, where exact results are obtained. Further, the applicability of the concept is investigated for an arbitrary infrastructure system. Finally, a conclusions and outlook are presented.

2 Theoretical Fundamentals

2.1 Structure Function

According to [35], the performance of a system depends only on its components, i.e., their states, and their interactions. Then, a vector $\boldsymbol{x}(t)$ can be seen as the component state vector of the system assigning a state to each component. $\boldsymbol{x}(t)$ should dependent on the environmental conditions. As a result, the system performance can be described as a function of the component state vector. Suppose that a component state is modeled via probability distributions in dependence on component properties, environmental effects, and time. Then, the system performance function solely describes the system structure, corresponding to the arrangement of the components and their interactions. Such a system performance model can be considered as the well-known system structure function. In the current work, the structure function is assumed to be time-independent.

2.1.1 Binary-State Structure Function

The structure function of a system is a fundamental concept to represent system topology in reliability analysis. For a binary-state system the structure function can be defined as follows. Let a system consist of n components of the same type. Further, let $\boldsymbol{x} = (x_1, x_2, \ldots, x_n) \in \{0,1\}^n$ be the corresponding state vector of the n components, where $x_i = 1$ indicates a working state of the i-th component and $x_i = 0$ indicates a nonworking state. Then, the structure function ϕ is a function of the state vector defining the operating status of the considered system:

$$\phi := \phi(\boldsymbol{x}) : \{0,1\}^n \to \{0,1\}, \tag{1}$$

as proposed, e.g., in [26] Accordingly, $\phi(\boldsymbol{x}) = 1$ denotes a working system and $\phi(\boldsymbol{x}) = 0$ specifies a nonworking system relative to the state vector $\boldsymbol{x}$.

Let a system consist of components of different types, i.e., $K \geq 2$. Then, the number of system components is denoted by $n = \sum_{k=1}^{K} n_k$, where n_k is the number of components of type $k \in \{1, 2, \ldots, K\}$. Accordingly, the state vector for each type is specified by $\boldsymbol{x}_k = (x_{k,1}, x_{k,2}, \ldots, x_{k,n_k})$.

2.1.2 Multi-State Structure Function

Analogously, the structure function can be defined for a discrete multi-state consideration. Then, the system and component states degrade from a perfect state over a set of intermediate states to the state of complete failure:

$$\phi := \phi(\boldsymbol{x}) : \{0, \ldots, M\}^n \rightarrow \{0, \ldots, M\}, \tag{2}$$

compare [36].

2.1.3 Continuous-State Structure Function

When following a continuous multi-state consideration, the set of possible system and component states are all elements of the interval between 0 and 1. Such a consideration relates to the performance function well-known in structural reliability when normalized for minimum and maximum parameter values, e.g., as proposed in [37]:

$$\phi := \phi(\boldsymbol{x}) : [0, 1]^n \rightarrow [0, 1]. \tag{3}$$

2.2 Coherent System

A special case of the general system is the class of coherent systems. Note that binary-state, discrete multi-state, as well as continuous multi-state structure functions can be coherent. In accordance with Hudson & Kapur [38], this class can be defined as follows. A (discrete or continuous multi-state) system is defined to be coherent if the three subsequent conditions are fulfilled:

- $\phi(\boldsymbol{x})$ is surjective. Consequently, for each system state m there exists at least one state vector $\boldsymbol{x}$ for which $\phi(\boldsymbol{x}) = m$.
- $\phi(\boldsymbol{x}) \leq \phi(\boldsymbol{y})$ if $\boldsymbol{x} \leq \boldsymbol{y}$, i.e., ϕ is monotone and non-decreasing.
- The set C of all components contains no inessential components, i.e., each component influences the system performance at some point.

2.3 Concept of Binary-State Survival Signature

The concept of the survival signature is a promising approach for a more efficient evaluation of system reliability, especially when it comes to repeated model evaluations. Introduced in [26], this concept enables to compute the survival function of a system. The approach attracted increasing attention over the last decade due to its advantageous features compared to traditional methods [27]. One of its benefits is the efficiency in repeated model evaluations due to a separation of the probability structure of system components and the topological system reliability. In addition, the survival signature significantly condenses information on the topological reliability for systems with multiple component types. Components are of the same type if their failure times are independent and identically distributed (*iid*) or exchangeable. This distinction is important when modeling dependent component failure times [39]. For more information on

claimed exchangeability in practice, see [39, 28]. In the following the derivation of the concept of survival signature is shown for a binary-state system with a single component type and multiple component types, respectively, based on Coolen et al. [26]. More detailed information about further applications and the derivation of the concept can be found in [26, 39, 40].

Consider a coherent system with a given structure function as described in subsubsection 2.1.1. Given a binary-state vector specifying the state of n components in total, there are $\binom{n}{l}$ state vectors $\boldsymbol{x}$ with exactly l components with $x_i = 1$, i.e., $\sum_{i=1}^{n} x_i = l$. Let the set of these state vectors refer to as S_l. Assume that the failure times of the components specifying $\boldsymbol{x}$ over time are *iid*. Consequently, all possible state vectors are equally likely to occur and, hence, it can be stated that

$$\Phi(l) = \binom{n}{l}^{-1} \sum_{\boldsymbol{x} \in S_l} \phi(\boldsymbol{x}), \tag{4}$$

where $\phi(\boldsymbol{x})$ is the binary-state structure function. Then, $\Phi(l)$ denotes the probability that a system is working given that exactly l of its components working for $l = 1, \ldots, n$. Note that the survival signature depends only on the topological reliability of the system, independent of the time-dependent failure behavior of its components, hereafter referred to as the probability structure of the system. It holds that $\Phi(0) = 0$ and $\Phi(n) = 1$ due to the coherent system property. The expression given in Equation 4 closely relates to the signature, introduced by Samaniego in [41].

The probability structure of system components specifies the probability that a certain number of components of type k are working at time t. Let $C_t \in \{0, 1, \ldots, n\}$ be the number of components functioning at time $t > 0$. Further, the probability distribution of the component failure time is described by the cumulative density function (CDF) $F(t)$. Therefore, the probability structure for $l \in \{0, 1, \ldots, n\}$ is given as

$$P\left(C_t = l\right) = \binom{n}{l} [F(t)]^{n-l} [1 - F(t)]^{l}. \tag{5}$$

The topological reliability described by Eqn. (4) and the probability structure characterizing the component failure times can be brought together to obtain the survival function as

$$R(t) = P\left(T_f > t\right) = \sum_{l=0}^{n} \Phi(l) P\left(C_t = l\right), \tag{6}$$

where T_f denotes the random system failure time. Clearly, the two terms on the right-hand side of the equation have different roles: The term $\Phi(l)$ represents the topological reliability and is determined by the structure function of the system, defining how the system functionality depends on the function of its components. The other term $P\left(C_t = l\right)$ describes component failure behavior and is referred to as the probability structure of the system. Consequently, the concept of survival signature separates the time-independent topological reliability and the time-dependent probability structure. Thus, the survival signature computed once in a preprocessing step can be reused for further evaluations of the survival function. The survival signature can be stored in a matrix, summarizing the topological reliability. The utilization of this matrix circumvents the repeated evaluation of the typically computationally expensive structure function. Note that precisely these properties give the concept of survival signature an advantage over conventional methods when system simulations must be performed repeatedly [27].

The survival function $R(t)$ is a well-known concept in reliability engineering that is also referred to as reliability function [42, 43]. It is typically interpreted as the mathematical formalization of the definition of reliability provided in section 1 and quantifies the system failure time to be greater or equal to t. It relates to the CDF $F(t)$ as $R(t) = 1 - F(t)$.

It is also possible to define the concept of survival signature for $K \geq 2$, with K being the number of component types. In this case, the survival signature summarizes the probability that a system is working as a function depending on the number of working components l_k for each type $k = 1, \ldots, K$, see [26] for more details.

2.4 Concept of Continuous-State Survival Signature

The original concept of survival signature achieves considerable efficiency advantages when computing system reliability but is limited to a binary-state consideration. However, a multi-state or even continuous-state consideration might be beneficial for the assessment of most real-world systems in terms of safety and cost efficiency. In the last years several researchers proposed various concepts that bring the survival signature to a multi-state consideration, see [31, 33, 34].

In [32], Liu et al. introduced an approach for the concept of survival signature in the context of continuous-state systems, for which the component functionality is characterized by a stress-strength relation. The strength of the components are assumed to be *iid*, while the strength X and the stress Y acting on the components are statistically independent. The state of a component is defined via a kernel function $K : \mathbb{R}^+ \to S$ through the relation $\eta = K(Z)$ with the random variable $Z = X/Y$. Thereby, $S \in \{0, 1, 2, \ldots, M\}$ and $S \in [0, 1]$, respectively, depending on a discrete or continuous multi-state consideration. The researchers provided formulas to compute the survival signature for discrete multi-state systems similar to [31] in a combinatorial manner but directly based on the number of path sets. Analogously, the survival signature for continuous multi-state systems is given as

$$\begin{aligned} \rho_{n_s}(n) &= P\left(\varepsilon \geq s \mid N(s,n) = n_s\right) \\ &= \delta_{n_s}(n) / \binom{n}{n_s} \end{aligned} \tag{7}$$

with

$$N(s,n) = \sum_{i=1}^{n} I(\eta \geq s) \tag{8}$$

that is the number of components in state s of in total n components and $\delta_{n_s}(n)$ being the number of path sets for which exactly n_s components are in state s or above. The time-independent probability that the system is at least in state s or above can then be given as

$$R(s) = \sum_{l_s=0}^{n} \rho_{l_s}(n) \binom{n}{l_s} P\left(N(s,n) = n_s\right), \tag{9}$$

where l_s is the number of components functioning in state s. Again, the left term represents the inherently time-independent topological reliability, while the right term refers to the probability structure that is time-independent in this case due to specific the stress-strength relation of components established in [32].

Despite an extension to discrete and continuous multi-state consideration, the authors limited their considerations in [32] to a time-independent reliability analyses. Thereby, $R(s)$ quantifies the probability that the entity under consideration performs in state s, compare $R(t)$ that measures the probability of the system failure time is greater or equal to time t. In addition, a stress-strength relation characterizing probabilistic properties of components must be established as prerequisite in order to determine the component probability structure $P\left(N(s,n) = n_s\right)$.

3 Proposed Methodology

In this section, the continuous-state survival function is defined. In contrast to the previously outlined approaches that are either probability measures of state s or time t, this notion depends on both s and t simultaneously. For comparison with the subsequently presented methodology, a true solution estimate based on MCS is proposed in order to evaluate the continuous-state survival function. Eventually, the DAS is introduced as surrogate model to compute the continuous-state survival function efficiently.

3.1 Continuous-State Survival Function

In this work, the probability $P(u_s \geq s|t)$ that the state of some entity under consideration u_s is greater or equal to s at given time t is referred to as the continuous-state survival function of this entity and is denoted by

$$R(s,t) = P(U_s \geq s|t). \tag{10}$$

Thereby, the continuous-state survival function constitutes a time-dependent probability measure that characterizes the distribution of performance states of the considered entity over time. From another perspective, the continuous-state survival function can be interpreted as

$$R(s,t) = P(U_t \geq t|s), \tag{11}$$

where U_t is the random variable characterizing the time to failure of the condition that the state of the entity is greater than s. Despite this perspective does not find application in this work, the consideration is decisive for the terminology. In fact, the original and well-known survival function can be extended to this notion when conditioning the considered lifetime to a state s in the interval $[0,1]$ instead of a binary condition of operating or not operating.

In the context of systems that consist of components facing disruptive events, the entity under consideration may correspond to either a system or one of its components. Thereby, $R(s,t)$ can be established in several ways. The first attempt to quantify $R(s,t)$ could be a fully empirical approach, measuring the frequency of the system or component state u_s. Given the typically limited number of samples, engineers in most cases face the challenge of modeling a stochastic process based on limited data or expert knowledge and to utilize it as basis for sampling performances as an alternative. Besides that, the continuous-state survival function can be evaluated based on a given structure function $\phi(\boldsymbol{x})$, as presented in subsection 2.1, that represents system topology, i.e., component interaction, and a given probability structure describing the degrading component performance over time. The latter approach involving $\phi(\boldsymbol{x})$ will be focal point for all subsequent developments.

Consider a system with a coherent and time-invariant structure function $\phi(\boldsymbol{x})$. Then $u_s = \phi(\boldsymbol{x})$ and the corresponding continuous-state survival function can be given by $R(s,t) = P(\phi(\boldsymbol{x}) \geq s|t)$. Figure 2 shows the contour line of an exemplary $2D$ system for a given state s. Thereby, $\partial\Omega_s := \{\boldsymbol{x} \mid \phi(\boldsymbol{x}) = s\}$ represents this contour line as the set of state vectors that meet exactly the system performance $\phi(\boldsymbol{x}) = s$ with $\boldsymbol{x} = (x_1, x_2, \ldots, x_n)$ and $x_i \in [0,1]$. $\Omega_s := \{\boldsymbol{x} \mid \phi(\boldsymbol{x}) \geq s\}$ corresponds to the set of state vectors that fulfill the criteria $\phi(\boldsymbol{x}) \geq s$. Given $\phi(\boldsymbol{x})$, an exact solution for $R(s,t)$ can be obtained by evaluating the integral of the time-dependent probability density at the state vectors belonging to Ω_s. Denote the underlying probability distribution as $f_{x_i}(x_i \mid t)$ – potentially time-dependent – describing the state x_i of component i. Further, let $\Omega = [0,1]^n$ be the set of all possible component states and assume the component states to be independently distributed. Then, the true solution of the

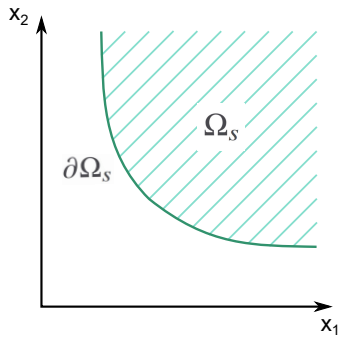

Figure 2: Examples for $\partial\Omega_s$ and Ω_s shown in a contour plot of an exemplary $2D$-system with the structure function $\phi(\boldsymbol{x})$ evaluated for an arbitrary state s.

continuous-state survival function is given as the integral over $\Omega_s \subseteq \Omega$:

$$\begin{aligned} R(s,t) &= \int_{\Omega_s} f_{\boldsymbol{x}}(\boldsymbol{x} \mid t) d\boldsymbol{x} \\ &= \int_{\Omega} I(\phi(\boldsymbol{x}) \geq s) f(\boldsymbol{x} \mid t) d\boldsymbol{x}, \end{aligned} \tag{12}$$

where $f_{\boldsymbol{x}}(\boldsymbol{x} \mid t) = \bigcap_{i=1}^{n} f_{x_i}(x_i \mid t)$ is the conditional joint probability density characterizing the probability of the component state vector $\boldsymbol{x}$. Further, $I(\cdot) \in \{0, 1\}$ denotes the indicator function.

In fact, the identification of $\partial\Omega_s := \{\boldsymbol{x} \mid \phi(\boldsymbol{x}) = s\}$, that corresponds to the well-known limit state function, in order to quantify the probability mass assigned to the elements in Ω_s is a challenging task, particularly for nonlinear functions. MCS is applied to obtain an estimate of the true solution, since there is no closed form available to solve this general and possibly multi-dimensional problem. It holds true that

$$\begin{aligned} R(s,t) &= \int_{\Omega} I(\phi(\boldsymbol{x}) \geq s) f_{\boldsymbol{x}}(\boldsymbol{x} \mid t) d\boldsymbol{x} \\ &= \frac{1}{N_{MCS}} \sum_{j=1}^{N_{MCS}} I(\phi(\boldsymbol{x}_j) \geq s \mid t), \end{aligned} \tag{13}$$

where N_{MCS} is the number of component state samples $\boldsymbol{x}_j \in \Omega \sim f_{\boldsymbol{x}}(\boldsymbol{x} \mid t)$ used for MCS, when $N_{MCS} \to \infty$.

3.2 Surrogate Model: The Concept of Diagonal Approximated Signature

The concept of the DAS is introduced as a surrogate modeling approach that enables the computation of the true continuous-state survival function or at least an approximation of it depending on the characteristics of $\phi(\boldsymbol{x})$. Similarly to the concepts of binary- and discrete/continuous multi-state survival signatures, the concept of the DAS is based on a decomposition of working components, compare l that is the number of components working, as in Equation 6, and l_s that is the number of components functioning in state s, as in Equation 9, respectively. This leads to a separation property of these concepts that enables to store information on the system topology, i.e., the functional interaction of components, and retrieve it in repeated model evaluations more efficiently than compared to the evaluation via the original structure function.

3.2.1 Fundamental Statement

With regard to the current developments, several categorizations for three properties of a coherent system structure function are introduced. As first property, the diagonal state sign can be defined: A coherent structure function is referred to as diagonally state positive if it holds that $\phi(x_s) > s \; \forall s \in [0,1]$ with $x_s = (x_1, x_2, \ldots, x_n)$ and $x_i = s$ where n is the number of system components. Analogously, the terms diagonally state neutral and diagonally state negative correspond to the conditions $\phi(x_s) = s$ and $\phi(x_s) < s$, respectively. Secondly, note that a structure function is called diagonally state invariant in particular if it is diagonally state neutral. In contrast, the property of the diagonal state variance can also be assigned as diagonally state variant if the structure function is partly diagonally state positive, neutral and negative. The third property can be assigned as diagonally state extreme if it holds that $\phi(x_s) \geq s \;\; \forall s \in [0,1]$ with $x_s = (x_1, x_2, \ldots, x_n)$ and $x_i \in \{0, s\}$. This condition would imply that the structure function is also diagonally state constant, i.e., $\phi(x_s) \geq s \;\; \forall s \in [0,1]$ with $x_s = (x_1, x_2, \ldots, x_n)$ and $x_i \in [0, s]$. Let these specifications relate to the diagonal state order. As an example, both of these properties can be specified as diagonally state neutral and diagonally state extreme for structure functions that are solely composed by min- or max-operators, i.e., compositions of $\phi_e(\boldsymbol{x}) = \min(x_f, x_g) \in [0,1]$ and $\phi_h(\boldsymbol{x}) = \max(x_j, x_k) \in [0,1]$ with $x_f, x_g, x_j, x_k \in [0,1]$. In addition to such systems, Liu et al. also investigated $k - consecutive - out - of - n - systems$ which are diagonally state neutral and diagonally state extreme, compare [32]. The min- and max-operators can be interpreted as analogy of series and parallel operators known from the binary-state consideration, as stated in[30]. The binary operators often appear in reliability block diagrams.

Assume a coherent structure function to be diagonally state neutral or at least positive and at least diagonally state constant. Then, the basic concept of the DAS can be stated as

$$\begin{aligned} R(s,t) &= \int_{\Omega_s} f_{\boldsymbol{x}}(\boldsymbol{x} \mid t)\, d\boldsymbol{x} \\ &= \sum_{l_s=0}^{n} \sum_{p=1}^{\binom{n}{l_s}} \left[R_x(\Phi(l_s,p) \mid t) - R_x(s \mid t)\right]^{n-l_s} \left[R_x(s \mid t)\right]^{l_s}, \end{aligned} \tag{14}$$

where $\Phi(l_s, p)$ represents the DAS and $R_x(s \mid t) = R_{x_i}(s \mid t) = P\{x_i \mid x_i \geq s, t\}$ corresponds to the probability that a component is in state s or above at time t given that all component states are *iid* or exchangeable. Thereby, $\Phi(l_s, p)$ stores values representing an approximation of the limit state function, i.e., $\partial\Omega_s$ that is the set of component state vectors fulfilling the condition $\phi(\boldsymbol{x}) = s$. For a given state s, the p-th permutation of the overall $\binom{n}{l_s}$ permutations defines a subspace $\Omega_{s,l_s,p} \subseteq \Omega_{s,l_s} \subseteq \Omega_s \subseteq \Omega$ determined by l_s that is the number of components working in state s. All state vectors in the set of $\Omega_{s,l_s,p}$ fulfill the condition $\phi(\boldsymbol{x}) \geq s$. Let the value of $\Phi(l_s, p)$ for subspace $\Omega_{s,l_s,p}$ be the minimum value of $n - l_s$ components of the state vector $\boldsymbol{x}$ in the interval $[0, s)^{n-l_s}$ for which the condition $\phi(\boldsymbol{x}) \geq s$ is met, while l_s components are fixed in state s. The developed algorithm for computing the values $\Phi(l_s, p)$ ensures that the continuous-state survival function $R(s,t)$ can only be underestimated in the worst case.

3.2.2 Derivation of the Fundamental Statement

The derivation of Equation 14 can be given as follows. Let $I = \{1, 2, \ldots, n\}$, where $n = |I|$, and $(k_1, k_2, \ldots, k_n) \in K_p \coloneqq \binom{I}{l_s}$. Then, K_p is the index set of all possible permutations of the state vector for a given number of components functioning in state s with in total $\binom{n}{l_s}$ elements, and the index $p \in \{1, 2, \ldots, \binom{n}{l_s}\}$ corresponds to the p-th permutation. At first, consider the

decomposition of Ω_s, the set of state vectors for which the condition $\phi(\boldsymbol{x}) \geq s$ is fulfilled, into its subspaces when given l_s components functioning in state s. The decomposition is formulated as

$$\begin{aligned}
\Omega_s = \{\boldsymbol{x} \mid \phi(\boldsymbol{x}) \geq s\} &= \bigcup_{l_s=0}^{n} \Omega_{s,l_s} = \Omega_{s,0} \cup \bigcup_{l_s=1}^{n-1} \Omega_{s,l_s} \cup \Omega_{s,n} \\
&= \bigcup_{p=1}^{\binom{n}{0}} \{x_{k_1}, \ldots, x_{k_n} < s \wedge \phi(\boldsymbol{x}) \geq s\} \\
&\quad \cup \bigcup_{l_s=1}^{n-1} \bigcup_{p=1}^{\binom{n}{l_s}} \left\{x_{k_1,\ldots,x_{k_i}} \geq s \wedge x_{k_{i+1}}, \ldots, x_{k_n} < s \wedge \phi(\boldsymbol{x}) \geq s\right\} \\
&\quad \cup \bigcup_{p=1}^{\binom{n}{n}} \{x_{k_1}, \ldots, x_{k_n} \geq s \wedge \phi(\boldsymbol{x}) \geq s\} \\
&= \bigcup_{l_s=0}^{n} \bigcup_{p=1}^{\binom{n}{l_s}} \Omega_{s,l_s,p},
\end{aligned} \tag{15}$$

where $\{k_{i+1}, \ldots, k_n\} = (I/K_p)$. Note that the subspace Ω_{s,l_s} is also decomposed into the subspaces $\Omega_{s,l_s,p}$ defined via all possible permutations p of the state vector for l_s given components functioning in state s or above and the corresponding $n - l_s$ components functioning in state $< s$.

Secondly, the set-theoretical decomposition $\bigcup_{l_s=0}^{n} \bigcup_{p=1}^{\binom{n}{l_s}} \Omega_{s,l_s,p}$ proposed in Equation 15 is utilized to decompose the time-dependent state probability and to separate the probability structure and the information on the limit state function. This spatial decomposition depending on a given state s and time t is now utilized to form sums of mutually exclusive event sets as:

$$\begin{aligned}
R(s,t) &= \int_{\Omega_s} f(\boldsymbol{x} \mid t)\, d\boldsymbol{x} \\
&= P(\Omega_s|t) = P(\bigcup_{l_s=0}^{n} \bigcup_{K_p=\binom{I}{l_s}}^{\binom{n}{l_s}} \Omega_{s,l_s,p}|t) \\
&= \sum_{l_s=0}^{n} \sum_{p=1}^{\binom{n}{l_s}} \int_{\Omega_{s,l_s,p}} f(\boldsymbol{x} \mid t)\, d\boldsymbol{x}.
\end{aligned} \tag{16}$$

The claim that the coherent structure function is diagonally state neutral or positive and at least diagonally state constant implies that $\Omega_{s,l_s,p} = [a_i(l_s,p), b_i(l_s,p)]^n$. The boundary points $a_i(l_s,p)$ and $b_i(l_s,p)$ characterize the subspace $\Omega_{s,l_s,p}$ and depend on l_s the number of components functioning in state s and the permutation p. Further, assume that the components are independent and identically distributed, i.e., $x_1, x_2, \ldots, x_n = x \sim f_x(x_i \mid t)$. Consequently,

it can be stated that

$$\begin{aligned}\int_{\Omega_{s,l_s,p}} f(\boldsymbol{x} \mid t)\, d\boldsymbol{x} &= \int_{\Omega_{s,l_s,p}} f_1(x_1 \mid t) f_2(x_2 \mid t) \cdots f_n(x_n \mid t)\, dx_1 dx_2 \ldots dx_n \\ &= \prod_{i=1}^{n} \int_{a_i(l_s,p}^{b_i(l_s,p)} f_i(x_i \mid t) dx_i = \prod_{i=1}^{n} \int_{a_i(l_s,p}^{b_i(l_s,p)} f_x(x_i \mid t) dx_i \\ &= \prod_{i=1}^{n} F_x(b_i(l_s,p) \mid t) - F_x(a_i(l_s,p) \mid t) \\ &= \prod_{i=1}^{n} 1 - R_x(b_i(l_s,p) \mid t) - (1 - R_x(a_i(l_s,p)) \mid t) \\ &= \prod_{i=1}^{n} R_x(a_i(l_s,p) \mid t) - R_x(b_i(l_s,p) \mid t).\end{aligned} \tag{17}$$

The expression proposed in Equation 14 involving the time-dependent state probability distribution results from Equation 17 when considering two reformulations: At first, note the simplification $R_x(a_j(l_s,p)) - R_x(b_j(l_s,p)) = R_x(s) - R_x(1) = R_x(s)$ for the j-th component of the overall $l_s \in \{0, 1, \ldots, n\}$ components functioning in state greater or equal to s. At second, it can be stated that the DAS $\Phi(l_s,p) = a_k(l_s,p)$ as $R_x(a_k(l_s,p)) - R_x(b_k(l_s,p)) = R_x(\Phi(l_s,p)) - R_x(s)$ for the k-th component of the overall $n - l_s$ components in state $< s$. Consequently,

$$\begin{aligned}\int_{\Omega_{s,l_s,p}} f(\boldsymbol{x} \mid t)\, d\boldsymbol{x} &= \prod_{i=1}^{n} R_x(a_i(l_s,p) \mid t) - R_x(b_i(l_s,p) \mid t) \\ &= [R_x(\Phi(l_s,p) \mid t) - R_x(s \mid t)]^{n-l_s} [R_x(s \mid t)]^{l_s}.\end{aligned} \tag{18}$$

Then, Equation 16 and Equation 18 are brought together to finally obtain the expression presented in Equation 14:

$$\begin{aligned}R(s,t) &= \sum_{l_s=0}^{n} \sum_{p=1}^{\binom{n}{l_s}} \int_{\Omega_{s,l_s,p}} f(\boldsymbol{x} \mid t)\, d\boldsymbol{x} \\ &= \sum_{l_s=0}^{n} \sum_{p=1}^{\binom{n}{l_s}} [R_x(\Phi(l_s,p) \mid t) - R_x(s \mid t)]^{n-l_s} [R_x(s \mid t)]^{l_s}.\end{aligned} \tag{19}$$

Note that the topological information captured beforehand in $\Phi(l_s,p)$ is then retrieved and inserted into the probability structure in order to evaluate $R(s,t)$.

3.2.3 Basic Algorithm for Evaluating the DAS

At a first attempt, the approximation of $\Phi(l_s,p)$ can be achieved via the numerical scheme proposed in Algorithm 1. The presented Algorithm 1 poses a basic optimization scheme for finding the values $\Phi(l_s,p)$ for given state s. The proposed algorithm yields an exact representation of the limit state function at state s if the coherent structure function is diagonally state extreme and an approximated representation for diagonally state constant systems.

Considering Algorithm 1, $\phi(\cdot)$ corresponds to the coherent structure function of the system and $\boldsymbol{x}_0 = (x_1, x_2, \ldots, x_n)$ with $x_i \in \{NaN, s\}$, where $\boldsymbol{x}_0$ contains l_s times s and $n - l_s$ times NaN. Further, s indicates the state under consideration. The tuple (l_s,p) is characterized by the number of components in state s and their arrangement in the vector $\boldsymbol{x}_0$. If the vector

Algorithm 1 Evaluation of $\Phi(l_s, p)$

function EVALUATEDIAGONALAPPROXIMATEDSIGNATURE($\phi(), \boldsymbol{x}_0, s, h_{max}$)

▷ fixed point evaluation

if $all(\boldsymbol{x}_0. == s)$ **then**
if $\phi(\boldsymbol{x}_0) \geq s)$ **then**
return s
end if
end if

▷ start iteration

$v, v_1 \leftarrow s$ ▷ initialize auxiliary iteration variables
$h \leftarrow 0$ ▷ initialize iteration counter
$systemstate \leftarrow \phi(\text{DETERMINESTATEVECTOR}(\boldsymbol{x}_0, v_1))$
while $h \leq h_{max}$ **do**
if $systemstate < s$ **then**
$v_1 \leftarrow v - \frac{s}{2^h}$
else if $systemstate \geq s$ **then**
$v \leftarrow v_1$
$v_1 \leftarrow v - \frac{s}{2^h}$
end if
$systemstate \leftarrow \phi(\text{DETERMINESTATEVECTOR}(\boldsymbol{x}_0, v_1))$
$h \leftarrow h + 1$
end while
return v_1
end function

▷ auxiliary function

function DETERMINESTATEVECTOR($\boldsymbol{x}_0, v_1$)
return $fill(\boldsymbol{x}_0[\boldsymbol{x}_0. == NaN], v_1)$
end function

$\boldsymbol{x}_0 = (x_1, x_2, \ldots, x_n)$ with $x_i = s$ fulfills the condition $\phi(\boldsymbol{x}_0) \geq s$, the structure function is at least diagonally state neutral for the given state s and s can be returned as value for $\Phi(l_s, 1)$ with $l_s = n$. For every other vector, the algorithm starts its search at s, next it checks the minimum value 0 and than evaluates the interval in between until it stops. The algorithm stops when meeting the condition $\phi(\boldsymbol{x}_0) = s$ or after a specified number of iterations h_{max}. Thereby, the step size is reduced in each iteration by 1/2 and the last value v that met the requirement $\phi(\textsc{DetermineStateVector}(\boldsymbol{x}_0, v_1)) \geq s$ is maintained and candidates are rejected if $\phi(\textsc{DetermineStateVector}(\boldsymbol{x}_0, v_1)) < s$. The Algorithm 1 yields exact results if the system is diagonally state extreme, since both extreme cases, i.e., $\Phi(l_s, p) = s$ and $\Phi(l_s, p) = 0$, are evaluated. For diagonally state constant structure functions the iteration achieves an underestimating approximation with an accuracy depending on h. The algorithm can be further improved by including the stopping criteria for a sufficiently small improvement between h and $h + 1$.

3.2.4 Extended Statements

Equation 14 and Equation 19, respectively, as well as the Algorithm 1 form the basis for all further developments of the concept of DAS. However, the established expression still appears to be computationally expensive, as the sum over all permutations becomes increasingly demanding for systems comprising a large number of components. Therefore, a naive approach is introduced based on counting the occurrences of equal values of $\Phi_c(l_s, p)$ in the subspace Ω_{s,l_s} to further reduce the computational effort: Let $\Psi(l_s, j) = (|C_j|, v_j)$ be the so-called condensed DAS that assigns a tuple for $l_s \in \{0, 1, \ldots, n\}$ and $j \in \{1, 2, \ldots, J\}$, where J is the number of unique values v_j of $\Phi(l_s, p)$ for a fixed l_s and $p \in \{1, 2, \ldots, \binom{n}{l_s}\}$. Thereby, v_j indicates the j-th unique element in the set C_j that is formally defined as $C_j \coloneqq \{(l_s, p) : \Phi(l_s, p) = v_j\}$. Then,

$$\begin{aligned} R(s,t) &= \sum_{l_s=0}^{n} \sum_{p=1}^{\binom{n}{l_s}} [R_x(\Phi(l_s,p) \mid t) - R_x(s \mid t)]^{n-l_s} [R_x(s \mid t)]^{l_s} \\ &= \sum_{l_s=0}^{n} \sum_{j=1}^{J} \Psi(l_s,j)[1] \, [R_x(\Psi(l_s,j)[2] \mid t) - R_x(s \mid t)]^{n-l_s} [R_x(s \mid t)]^{l_s} \\ &= \sum_{l_s=0}^{n} \sum_{j=1}^{J} |C_j| \, [R_x(v_j \mid t) - R_x(s \mid t)]^{n-l_s} [R_x(s \mid t)]^{l_s}. \end{aligned} \tag{20}$$

For most systems, the application of Equation 20 will lead to a tremendous reduction of computational cost since typically $J << |\{(l_s, p)\}|$ for a fixed l_s and $p \in \{1, 2, \ldots, \binom{n}{l_s}\}$.

For systems with high $|C_j|$ per l_s but many values of $v_j \in [0, 1]$ in direct neighborhood to each other, v_j can be rounded up for r digits. Formally, this is defined as $C_{j,r} \coloneqq \{(l_s, p) : \Phi(l_s, p) = v_{j,r}\}$, where $v_{j,r}$ is a rounded value of v_j up to r-th digit. Correspondingly, $\Psi_r(l_s, j) = (|C_{j,r}|, v_{j,r})$. Considering the Algorithm 1, the corresponding values $\Phi(l_s, p)$ were evaluated during the iteration and yield an approximation. This introduces an approximation error and a trade-off between computational cost and accuracy has to be made. The continuous-state survival function will be underestimated in the worst case, since $v_{j,r} > v_j \Rightarrow R(v_{j,r}) - R(s) \leq R(v_j) - R(s)$. Consequently, the concept of DAS can be formulated as an inequality for at least diagonally state neutral coherent structure functions that are not diagonally state constant. For such systems a subspace of $\Omega_{s,l_s,p}$ might be neglected. The hypervolume that is neglected and consequently by which the continuous-state survival function is underestimated depends on the shape and curvature of the corresponding limit state function. This probably large-scale

approximation error results from the facts that these systems are no longer diagonally state constant and the DAS values are evaluated along the state diagonals of the individual subspaces $\Omega_{s,l_s,p}$. Nevertheless, an underestimation of the continuous-state survival function is provided in the worst case. This property is of crucial importance in engineering practice to prevent an unconscious risk from being taken. Let the following inequality be referred to as the concept of the naive first-order DAS. It holds true that

$$\begin{aligned} R(s,t) &\geq \sum_{l_s=1}^{n} \sum_{p=1}^{\binom{n}{l_s}} [R_x(\Phi(l_s,p) \mid t) - R_X(s \mid t)]^{n-l_s} [R_x(s \mid t)]^{l_s} \\ &\geq \sum_{l_s=0}^{n} \sum_{j=1}^{J} \Psi_r(l_s,j)[1] \, [R_x(\Psi_r(l_s,j)[2] \mid t) - R_x(s \mid t)]^{n-l_s} [R_x(s \mid t)]^{l_s}, \end{aligned} \tag{21}$$

where $R_x(s \mid t) = R_{x_i}(s \mid t) = P\{x_i \mid x_i \geq s, t\}$, i.e., all component states are *iid*. The statement above refers to as first-order approach since higher-order approaches are plausible. One could consider convolutions of subspaces via a recursive formula. Let $\Phi^1(l_s,p)$ denote the first-order DAS. Then, statements involving higher-order DAS such as $\Phi^h(l_s,p)$ would rely on the subordinate values $\Phi^{h-1}(l_s,p)$. However, the development of such higher-order schemes is beyond the scope of this paper.

4 Case Studies

In this section, various system models are established that are designed for a proof of concept and a test of applicability of the developed approaches. Subsequently, the numerical results are presented.

4.1 System Structure Functions

Here, the structure functions are presented that will be studied to achieve a proof of concept and test the applicability of the approach. Note that the structure functions model the system topology, i.e., the functional interaction of components with each other.

4.1.1 Proof of Concept: Min- and Max-Systems

The min- and the max-operator are crucial in the context of continuous-state system reliability as these correspond to the fundamental series- and parallel-operator well-known from the binary-state consideration of system functionality. Typically, they appear in the context of reliability block diagrams. Several systems composed by these operators are established in order to proof the fundamental methodologies proposed in section 3. The following coherent structure functions composed by min- and max-operators are considered:

- 2-Component-Min-System

  The system is composed by two continuous-state components with $x_i \in [0,1]$. The components are linked by a min-operator. Both components are considered to be of the same type. The 2-Component-Min-System can be interpreted as the analog to a series-connection in the binary-state case. The structure function $\phi(\boldsymbol{x}) \in [0,1]$ can be defined in a functional form as

  $$\phi(\boldsymbol{x}) = min(x_1, x_2). \tag{22}$$

  This structure function is diagonally state neutral, consequently, also diagonally state invariant, and diagonally state extreme. A graphical representation is given in Figure 3.

Figure 3: System composed by a min-operator with two components.

- 2-Component-Max-System

  The system is composed by two continuous-state components with $x_i \in [0, 1]$. The components are linked by a max-operator. Both components are considered to be of the same type. The 2-Component-Max-System can be interpreted as the analog to a parallel-connection in the binary-state case. The structure function $\phi(\boldsymbol{x}) \in [0, 1]$ can be defined in a functional form as

$$\phi(\boldsymbol{x}) = max(x_1, x_2). \tag{23}$$

  This structure function is diagonally state neutral, consequently, also diagonally state invariant, and diagonally state extreme. A graphical representation is given in Figure 4.

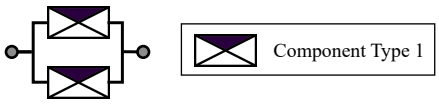

Figure 4: System composed by a max-operator with two components.

- 8-Component-MinMax-System

  The system is composed by eight continuous-state components with $x_i \in [0, 1]$. The components are linked by min-operators, as well as, max-operators. All components are considered to be of the same type. This system can be interpreted as the analog to a reliability block diagram that is composed by eight components. The structure function $\phi(\boldsymbol{x}) \in [0, 1]$ can be defined in a functional form as

$$\phi(\boldsymbol{x}) = max(min(max(x_1, x_2, x_3), x_5, x_8), min(x_4, max(x_6, x_7))). \tag{24}$$

  This structure function is diagonally state neutral, consequently, also diagonally state invariant, and diagonally state extreme. A graphical representation is given in Figure 5.

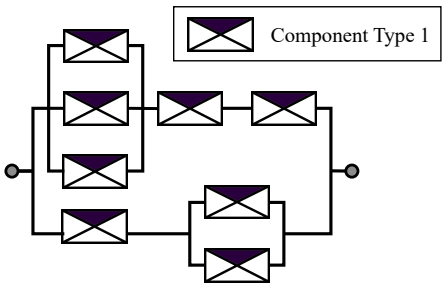

Figure 5: System composed by min- and max-operators with eight components, adapted from [25].

- 21-Component-MinMax-System

  The system is composed by 21 continuous-state components with $x_i \in [0, 1]$. The components are linked by min-operators, as well as, max-operators. All components are

considered to be of the same type. This system can be interpreted as the analog to a reliability block diagram that is composed by 21 components. The structure function $\phi(\boldsymbol{x}) \in [0, 1]$ can be defined in a functional form as

$$\begin{aligned}\phi(\boldsymbol{x}) =& min(max(min(x_1, max(x_6, x_7)), min(max(x_2, x_3), min(max(x_4, x_5),\\ & max(x_6, x_7)), x_8)), max(min(max(x_9, x_{10}), max(x_{14}, x_{15}, x_{16})),\\ & max(min(max(x_{11}, x_{12}), x_{17}), min(x_{13}, max(x_{18}, x_{19})))), max(x_{20}, x_{21})).\end{aligned} \tag{25}$$

This structure function is diagonally state neutral, consequently, also diagonally state invariant, and diagonally state extreme. A graphical representation is given in Figure 6.

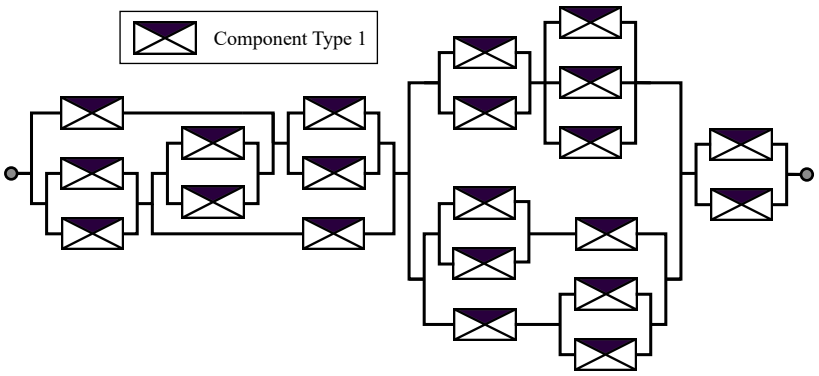

Figure 6: System composed by min- and max-operators with 21 components, adapted from [25].

4.1.2 Test of Applicability: Infrastructure System

In today's highly developed world, complex systems such as infrastructure networks and industrial plants are omnipresent and of vital importance to the functioning of modern societies. Consequently, the resilience of these systems is of utmost importance as well. Therefore, in the following, an arbitrarily chosen infrastructure network, represented by a graph, is considered. Figure 7 illustrates the graph of this exemplary system. Hereafter, This system is referred to as 18-Component-Infrastructure-System.

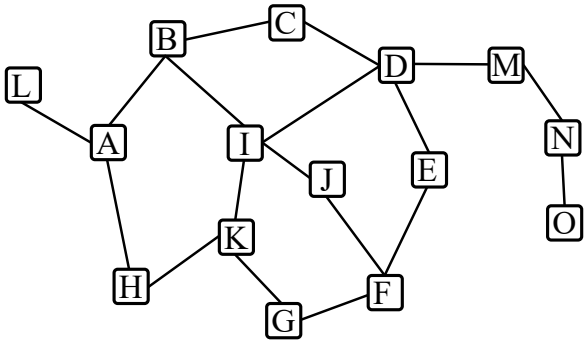

Figure 7: Arbitrary infrastructure system.

The graph consists of 15 nodes (capital letters, e.g., A) and 18 weighted edges (links between, e.g., $A - B$), where the nodes may represent cities in the system and the edges may represent transit links, as an example. The weights of the traffic routes can be interpreted as the travel time T required to complete this route.

As, e.g., in [44], [17] and [25], for the analysis of this infrastructure system it is assumed that it has a performance function defined by the so-called network efficiency. According to Latora and Marchiori [45], the network efficiency E represents a qualitative indicator of the connectivity of a network and is defined as:

$$E(G) = \frac{1}{N(N-1)} \sum_{i \neq j \in V} \frac{1}{d_{ij}^W}, \tag{26}$$

with G denoting the considered graph, V is the set of nodes, i.e., cities, $N = |V|$ the number of cities and d_{ij}^W the weighted path length between city i and city j, that is, the path with shortest travel time between these two cities. A detailed review of algorithms for efficiently determining the path length d_{ij}^W, such as the Floyd, Dijkstra, or Bellman-Ford algorithms, can be found, e.g., in [46] and [47]. Furthermore, the authors in [45] and [48] proposed the utilization of a normalized network efficiency E_{glob}:

$$E_{\text{glob}}(G) = \frac{E(G)}{E\left(G^{\text{ideal}}\right)}. \tag{27}$$

$E\left(G^{\text{ideal}}\right)$ is here the network efficiency of the graph in ideal state, i.e., all edges and nodes are present and fully operative. As a basis for calculating d_{ij}^W with respect to degrading edges, assume a monotonic functional relationship between the performance of the degrading edge and the travel time assigned to that edge. Therefore, a transformation function that maps

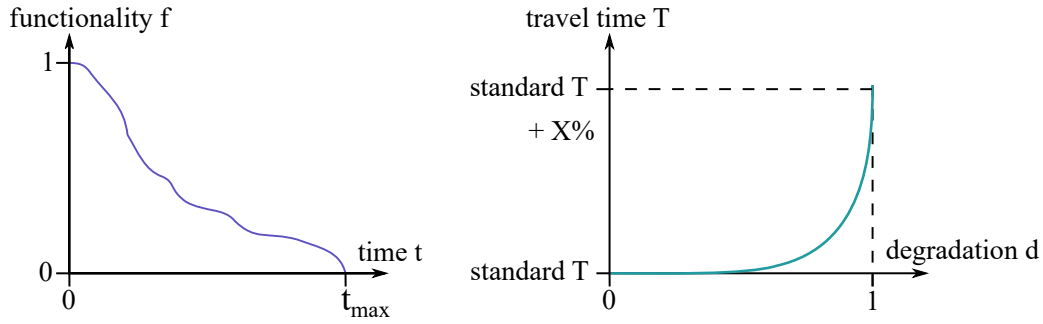

Figure 8: Relation of the edge degradation and travel time T for infrastructure graph systems.

the component functionality $f \in [0, 1]$ to a component degradation $d \in [0, 1]$ via $d = 1 - f$ is introduced. Further, the component degradation is mapped to the travel time T via an arbitrary function depicted in Figure 8 on the right. Note that the function has to ensure the requirement that the system structure function is at least diagonally state neutral. This function has an exponential shape, For $d = 0$, the travel time of the edge is equal to the standard travel time assigned as weight to the edge beforehand. The travel time increases up to a value of standard travel time plus 800% of the standard travel time as maximum.

4.2 Stochastic Modeling of the Component Degradation Process

As fundamental step for computing the continuous-state survival function via a structure function $\phi(\boldsymbol{x})$, the probability structure characterizing the component state vector $\boldsymbol{x}$ in a probabilistic manner over time has to be established. In the case of the DAS, this corresponds to the continuous-state survival function, while sampling during MCS requires probability densities as fundamental form. As outlined in subsection 3.1, there exist a variety of approaches to generate

the basic probability structure. In this work, an arbitrary stochastic process is proposed for illustrative purposes.

The stochastic degradation of components is modeled by combining an inverse Gamma process and a Gamma process. These types of processes are widely spread in stochastic degradation modeling [49, 50, 51]. Correspondingly, let $Z \sim InverseGamma(\alpha, 1)$ and $Y \sim Gamma(\beta, 1)$ be the random variables. Then, a random variable characterizing component degradation following a Beta process results when sampled as

$$X = \frac{Z}{Z+Y} \sim Beta(\alpha, \beta), \tag{28}$$

see [52].

MCS is applied to obtain a true solution estimate. In this case, the *iid* component state vector $\boldsymbol{x} = [0,1]^n$ is sampled with respect to Equation 28 for all obtained numerical results that are subsequently presented. Consequently, the state of the i-th component is characterized as $x_i = X$. Thereby, N_{MCS} state samples are generated for each component in the online phase.

In the case of the DAS, a continuous-state survival function describes the probabilistic characteristics of a component. Accordingly, the continuous-state survival function of a component can be established by solving the integral

$$R_x(s,t) = P(X \geq s \mid t) = \int_X I(X \geq s \mid t) = \frac{1}{N_{DAS}} \sum_{j=1}^{N} I(x_j \geq s \mid t), \tag{29}$$

where X denotes the random peformance variable characterizing the component state, I corresponds to the indicator function, s is the considered state threshold, and t corresponds to the currently considered time. Further, N_{DAS} refers to the number of MCS samples utilized to estimate the true solution of the continuous-state survival function for components and x_j is the j-the state sample, compare Equation 13. It is possible that $N_{DAS} \neq N_{MCS}$.

As exemplary parameters, $\alpha = 0.15$ and $\alpha = 0.6$ were arbitrarily selected. Further, $InverseGamma(\alpha, 1.5)$ was assumed, skewing the Beta process to the left. These parameters were applied for all presented case studies.

4.3 Numerical Results

In this section all computed results are presented. Convergence studies for the number of samples as well as studies concerning the computation time with respect to the number of samples and the number of states were conducted. Further, contour plots of the continuous-state survival function approximated by the DAS and contour plots depicting the corresponding error are provided. Note that the code utilized to compute the following numerical results was not optimized in terms of computational efficiency for the DAS and included *print* statements for computations based on MCS and DAS. Further, the code was not parallelized and variations in the capacity of working memory were unavoidable during the studies concerning convergence and computation time. Besides the study of computation time in terms of the number of considered states, all plots were generated with this number set to 101 states.

4.3.1 2-Component-Min-System

At first, consider the results computed for the continuous-state survival function of the 2-Component-Min-System. In Figure 9, the approximation of the continuous-state survival function by means of the concept of DAS is depicted. The contour plot shows $R(s,t)$ with a step size of 0.1. In this example, the sample size $N = N_{MCS} = N_{DAS}$ equals 51 000. No significant

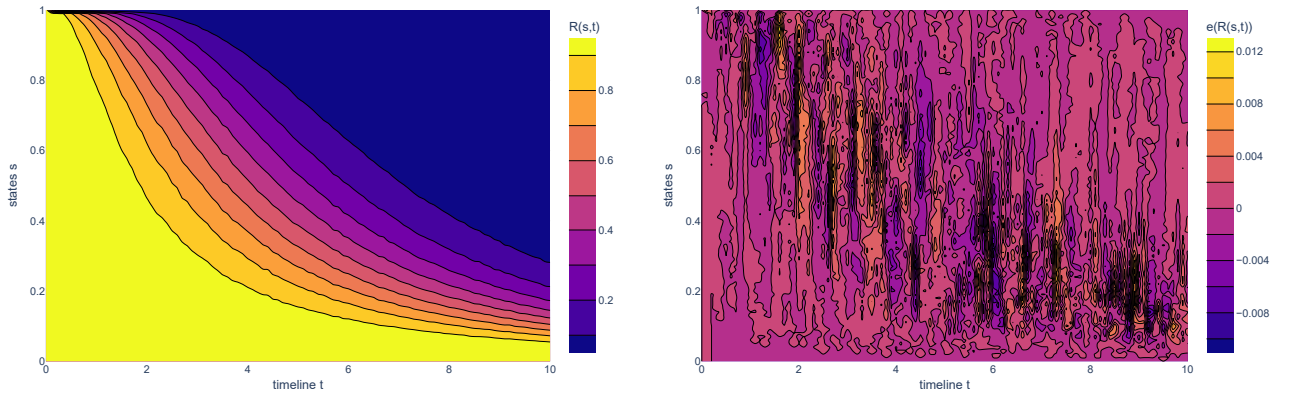

(a) Continuous-state survival function by means of DASC.

(b) Error between MCS estimate and DASC approximation.

Figure 9: 2-Component-Min-System: DAS condensed approximation of continuous-state survival function and the corresponding error.

differences between the computation via MCS, DAS and condensed DAS (indicated by DASC) could be observed during the study. Consequently, it is sufficient to consider a single contour plot out of three. As it can be observed in the figure, slight variations occur along the contour curves. Figure 9b shows the error between the true solution estimate obtained by means of MCS and the approximation via the condensed DAS. In theory, the DAS should yield exact results when for the underlying sampling process $N_{DAS} \to \infty$. This can be verified by the obtained results, as contour plot of the error purely exhibits variations with a maximum magnitude of 0.012 due to the variance in sampling process of the underlying component degradation. It can be presumed that the error vanishes completely for $N_{MCS} = N_{DAS} \to \infty$.

This becomes even more evident when considering Figure 10. The convergence study was conducted for sample sizes in the interval $[1\,000, 51\,000]$ with a step size of 10 000. Three different error measures were taken into account, namely, the Mean Absolute Error (MAE), the Mean Squared Error (MSE), and the Root Mean Square Error (RMSE). Thereby, the errors between MCS true solution estimate and both the approximations via DAS and via condensed DAS were considered. They represent the total error over the entire spatial and temporal domain under consideration. The error norms are common measures for evaluating the performance of estimators such as the MCS. As expected, all indicators converge against zero for an increasing sample size. The results emphasize that the developed approach neither suffers from significant outliers nor a bad approximation in average. Figure 11 shows studies concerning the computation time with respect to the number of samples N, see in Figure 11a, as well as to the number of considered states, see Figure 11b. The study with respect to sample size were considered analogously to the convergence study with sample sizes N_{MCS} and N_{DAS} between 1 000 and 51 000 with a step size of 1 000. For the study of computation time in terms of the number of considered states, the sample size N was set to 11 000. It can be observed that the MCS exhibits a steep linear relation between the total computation time in the online phase and the number of samples as well as a similar factorized linear relation between the online computation time and the number of states. Both DAS and DASC are constant with respect to the sample size. A slight linear relation can be observed in the plot considering the number of states. In both plots the DAS and DASC exhibit computation time in the same magnitude around 0 that is lower than the one achieved by MCS already for $N = 1\,000$. This results from the fact that the sums over $n = 2$ and $\max(|\binom{n}{l_s}|) = 3$ for the DAS as well as $n = 2$

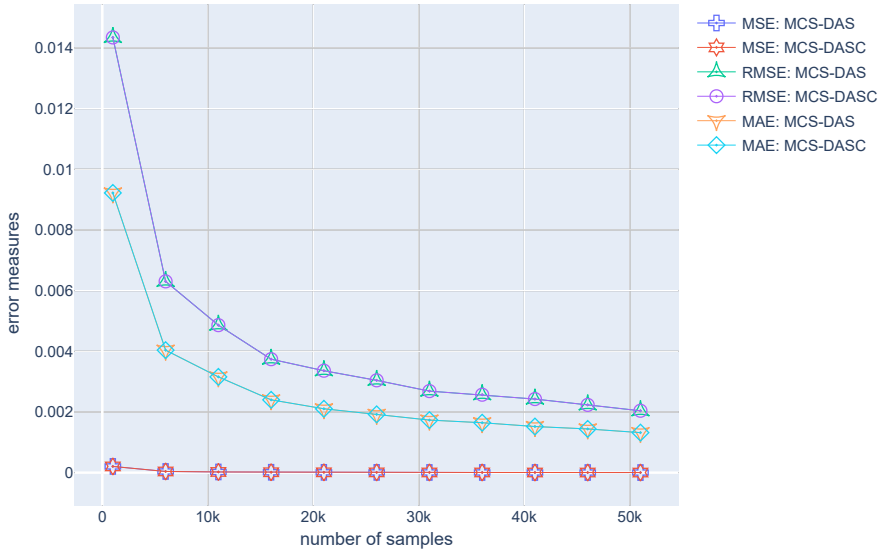

Figure 10: 2-Component-Min-System: Convergence study of MCS true solution estimate vs. DAS approximation of the continuous-state survival function with MAE, MSE and RMSE as error measures in terms of sample size N_{MCS}, while $N_{DAS} = 100\,000$.

and $J = 2$ for the DASC are computationally not demanding compared to 1 000 evaluations of the structure function.

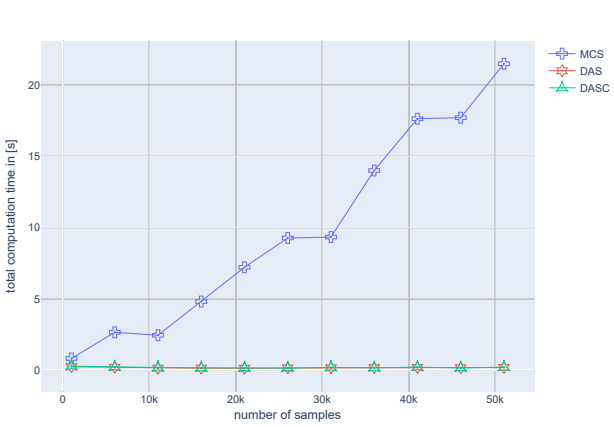

(a) ...with respect to the number of samples N.

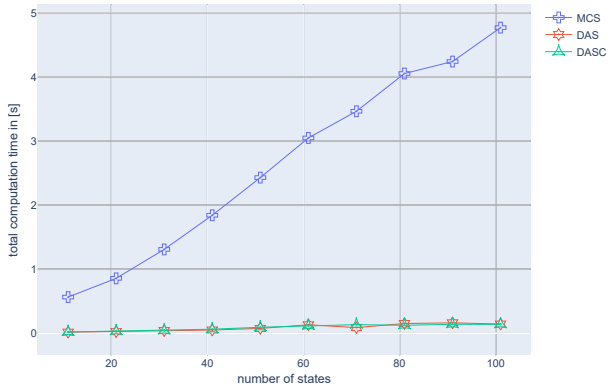

(b) ...with respect to the number of considered states.

Figure 11: 2-Component-Min-System: Study of computation time for MCS true solution estimate, DAS approximation, and DAS condensed approximation of the continuous-state survival function...

4.3.2 2-Component-Max-System

Secondly, consider the computed results for the continuous-state survival function of the 2-Component-Max-System. Again, Figure 12 shows the approximation of the continuous-state survival function by means of the DASC while Figure 12b depicts the corresponding error.

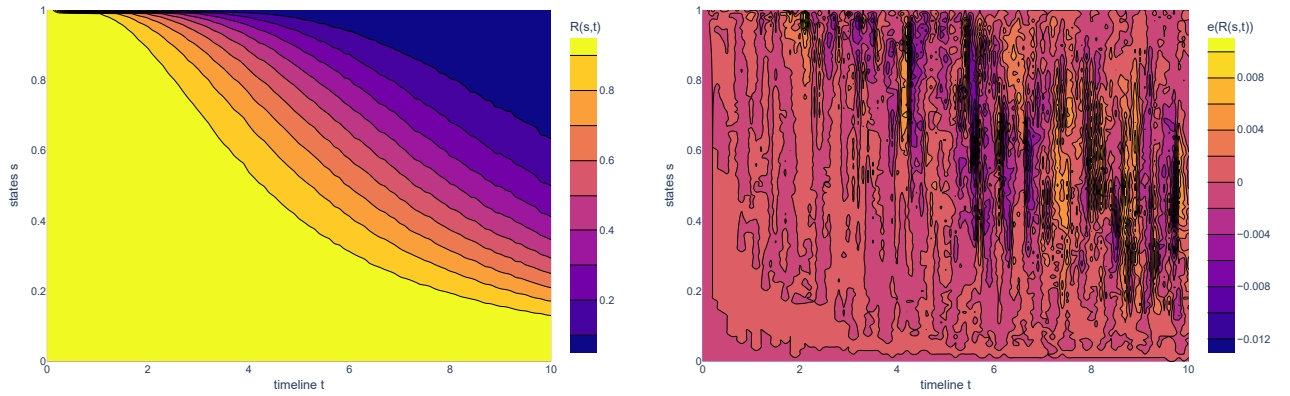

(a) Continuous-state survival function by means of DASC.

(b) Error between MCS estimate and DASC approximation.

Figure 12: 2-Component-Max-System: DAS condensed approximation of continuous-state survival function and the corresponding error.

Considering Figure 12a, the continuous-state survival function indicates higher reliability and robustness of the 2-Component-Max-System compared to the 2-Component-Min-System as expected. Not only is the domain for which $R(s,t) = 1$ larger but also the domain between the contour curves. In this example, the sample size $N = N_{MCS} = N_{DAS}$ equals 51 000. Similarly to the previous case study, slight variations occur along the contour curves. The error exhibits variations only due to the variance of the underlying sampling processes in the same magnitude of 0.012 as for the previous example.

Considering Figure 13 it becomes evident that also for this case study $e(R(s,t)) \to 0$ if $N_{DAS} \to \infty$. The results, obtained for all error measures, are as expected and similar to the previous case study. With regard to Figure 14, the sample sizes for both studies of computation time, compare Figure 14a and Figure 14b, are the same as in the previous example. Besides larger variations due to the in time varying capacity of the local working memory, the computation time required in the online phase are similar to the previous example. The MCS exhibits a linear relation for both sample size and number of states. In contrast, the DAS and DASC shows a constant relation, see Figure 14a. In terms of increasing states, a slight linear relation with significantly lower computation times can be observed, as illustrated in Figure 14b.

4.3.3 8-Component-MinMax-System

Again, Figure 15 verifies the expected behavior of the DAS and the DASC. In this example, the sample size $N = N_{MCS} = N_{DAS}$ equals 51 000. The contour plot of the continuous-state survival function in Figure 15a appears as a mixture of an 8-Component-System solely composed by min-operators as minimum and an 8-Component-System solely composed by max-operators. The error in Figure 15a has the same maximum magnitude of 0.0012 as in the previous examples. The region with the largest errors lies between the contour curves with $R(s,t) < 1$ and $R(s,t) > 0$. Considering the previous contour plot of the error, this high magnitude region shifts to the bottom left for a Min-System and to the upper right for a Max-System.

When considering Figure 16, the behavior of all three error measures appears similar to the previous examples. This is counterintuitive as one would expect an increasing error when

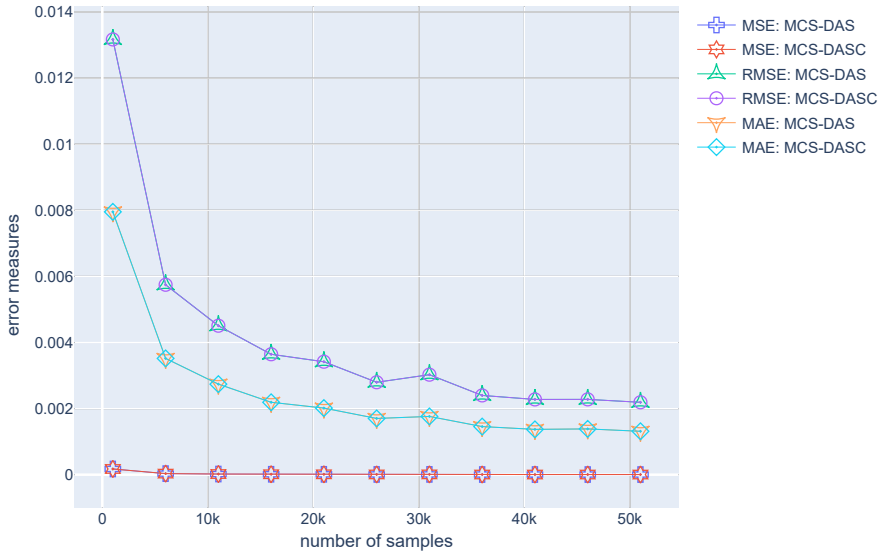

Figure 13: 2-Component-Max-System: Convergence study of MCS true solution estimate vs. DAS approximation of the continuous-state survival function with MAE, MSE and RMSE as error measures in terms of sample size N_{MCS}, while $N_{DAS} = 100\,000$.

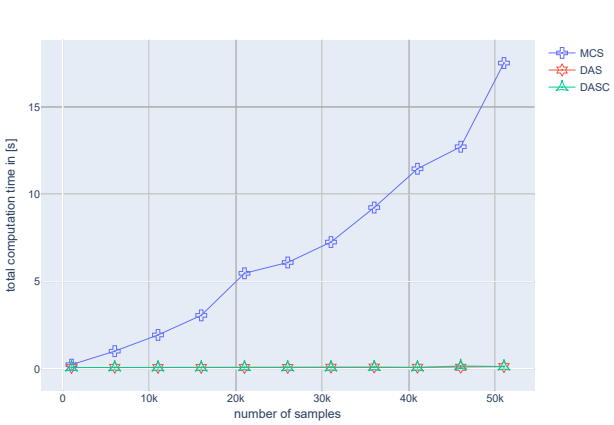

(a) ...with respect to the number of samples N.

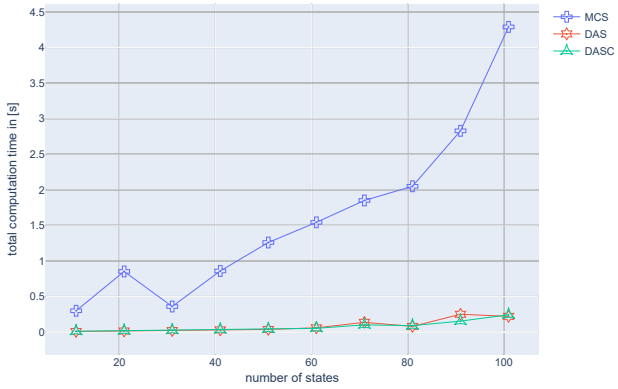

(b) ...with respect to the number of considered states.

Figure 14: 2-Component-Max-System: Study of computation time for MCS true solution estimate, DAS approximation, and DAS condensed approximation of the continuous-state survival function...

sampling in higher dimensions, compare [53]. But this seems not to hold true for diagonally state invariant structure functions. The ranges of sample sizes for both studies of computation time shown in Figure 17 are the same as in the previous example. Analogously to the previous examples, the computation times of the MCS are characterized by a similar linear relation with respect to both sample size and number of considered states. In contrast, DAS and DASC are constant in their relation with respect to the sample size. In terms of the number of considered state, both DAS and DASC follow linear relations. It is noteworthy, that the factor of the linear relation of the DAS seems significantly larger than before. Also in terms of the

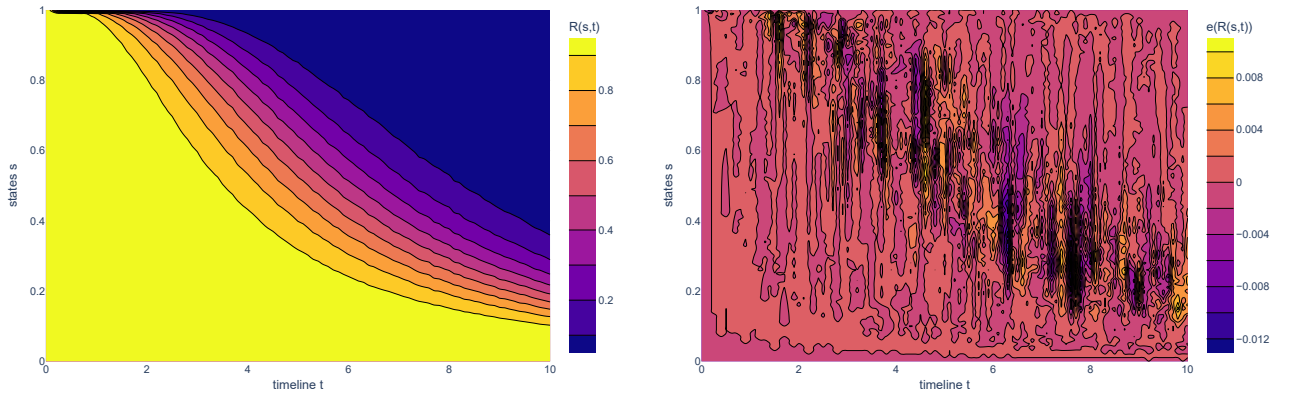

(a) Continuous-state survival function by means of DASC.

(b) Error between MCS estimate and DASC approximation.

Figure 15: 8-Component-MinMax-System: DAS condensed approximation of continuous-state survival function and the corresponding error.

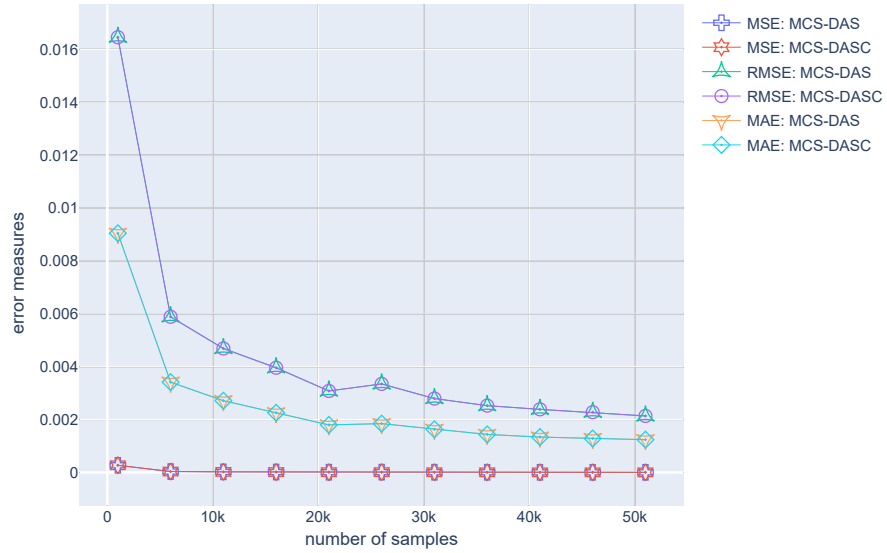

Figure 16: 8-Component-MinMax-System: Convergence study of MCS true solution estimate vs. DAS approximation of the continuous-state survival function with MAE, MSE and RMSE as error measures in terms of sample size N_{MCS}, while $N_{DAS} = 100\,000$.

sample size the computational time during the online phase significantly increased for the DAS. It can be observed that for $N = 1\,000$ the DAS is outperformed by the MCS approach. This result is reasonable as the number of permutations tremendously increase for higher dimensions corresponding to the binomial coefficient $\binom{n}{l_s}$, besides the already increasingly demandaning sum over n leading to the slightly increased linear relation of the DASC. Nevertheless, the DASC still possesses a low factor in its linear relation while maintaining exact results.

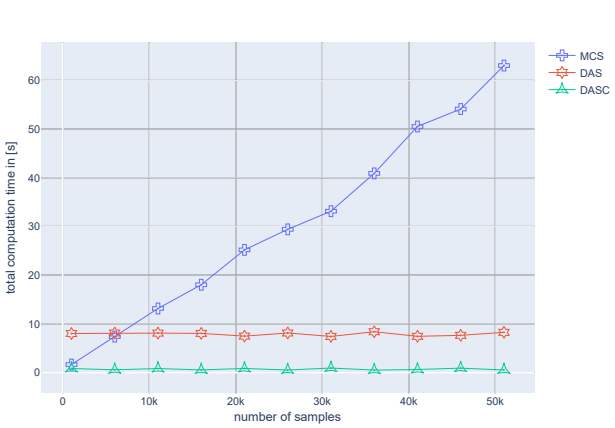

(a) ...with respect to the number of samples N.

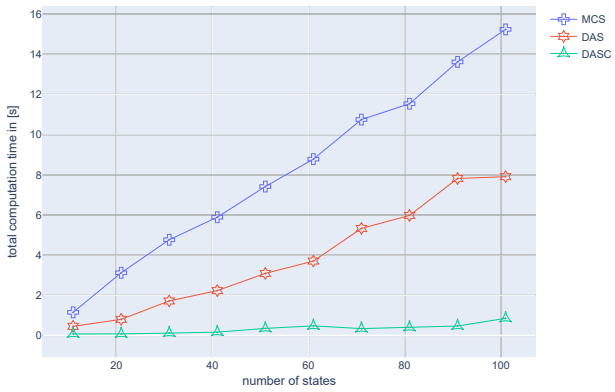

(b) ...with respect to the number of considered states.

Figure 17: 8-Component-MinMax-System: Study of computation time for MCS true solution estimate, DAS approximation, and DAS condensed approximation of the continuous-state survival function...

4.3.4 21-Component-MinMax-System

For this case study, the fundamental concept of DAS was omitted due to the combinatorial complexity of $\binom{n}{l_s}$ becoming computationally too demanding, resulting in unreasonable computational time. Consequently, solely the condensed DAS is applied as surrogate modeling

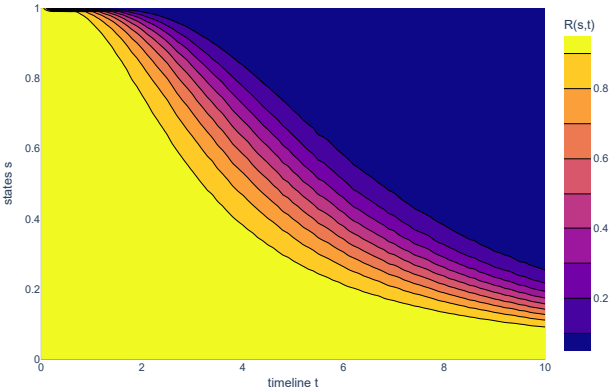

(a) Continuous-state survival function by means of DASC.

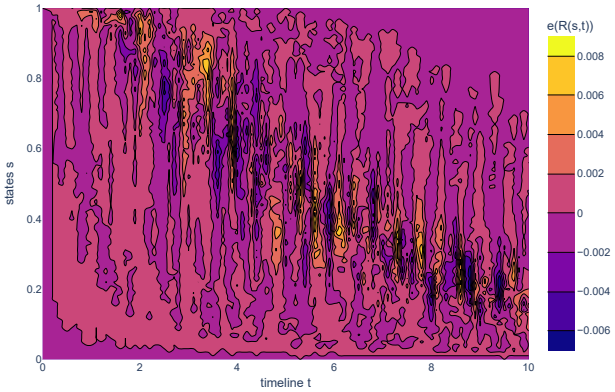

(b) Error between MCS estimate and DASC approximation.

Figure 18: 21-Component-MinMax-System: DAS condensed approximation of continuous-state survival function and the corresponding error.

approach. Considering Figure 18a and comparing it to the previous examples, the continuous-state survival function appears as a mixture of min- and max-operators as expected. It is observable that the domain in between of the contour curves are smaller than in the previous examples. In this example, the sample size $N = N_{MCS} = N_{DAS}$ equals 100 000. The sample size was increased to maintain a similar magnitude of errors as can be observed in Figure 18b.

For the convergence study depicted in Figure 19, the number of samples was increased for the entire range. The evaluated sample sizes lie in the interval $[20\,000, 200\,000]$ with a corresponding

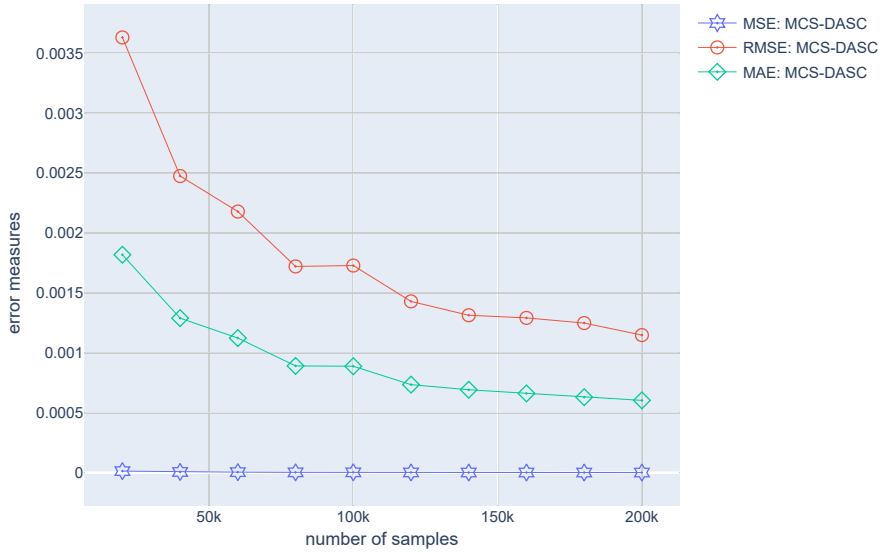

Figure 19: 21-Component-MinMax-System: Convergence study of MCS true solution estimate vs. DAS approximation of the continuous-state survival function with MAE, MSE and RMSE as error measures in terms of sample size N_{MCS}, while $N_{DAS} = 100\,000$.

step size of 20 000. The DASC also converges to zero for this high-dimensional structure function that is diagonally state neutral and diagonally state extreme as composed by min- and max-operators. This coincides with the theory established in section 3: The DAS and DASC yield the true solution of such systems or at least an estimate only in dependence on the variance of the underlying estimator of the component probability structure. For the study of computation

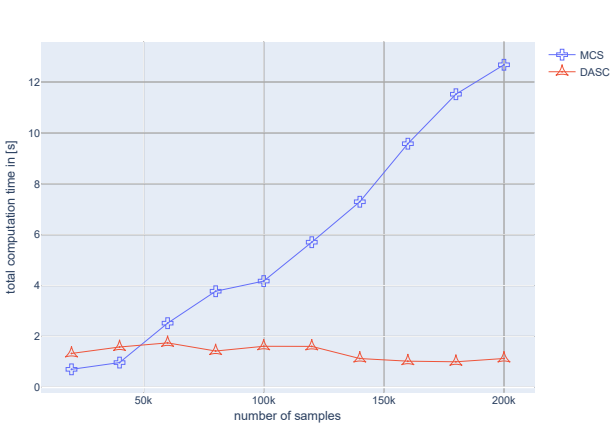

(a) ...with respect to the number of samples N.

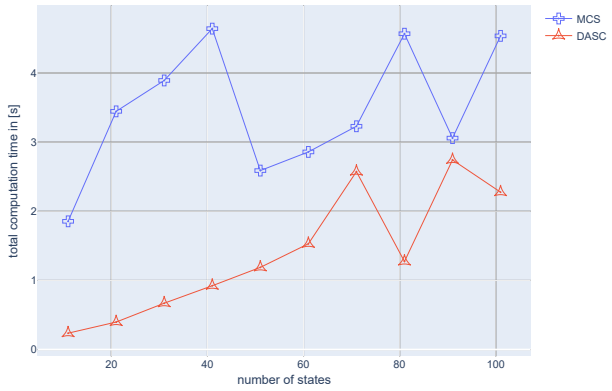

(b) ...with respect to the number of considered states.

Figure 20: 21-Component-MinMax-System: Study of computation time for MCS true solution estimate, DAS approximation, and DAS condensed approximation of the continuous-state survival function...

time regarding the number of considered states, the sample size N was set to 100 000. In terms of computation time, higher variance can be observed in Figure 20 then in the previous examples.

This relates to the variance in capacity of the deployed working memory. Again, a steep linear relation can be observed for the MCS in terms of an increasing sample size. The DASC exhibits a constant relation for N_{DAS} due to its independence. The expected linear relation of the DASC concerning the number of considered states significantly increased compared to the previous examples. Despite the tremendous increase of computational complexity, the DASC still outperforms the MCS globally. Only for smaller sample sizes where larger error magnitudes can be observed the MCS shows slightly shorter computation times compared to the constant.

4.3.5 18-Component-Infrastructure-System

For this example, solely the DASC and the rounded DASC (referred to as DASCR) were considered. To compute the underlying DAS for this example the maximum number of iteration steps h_{max} was set to 100.

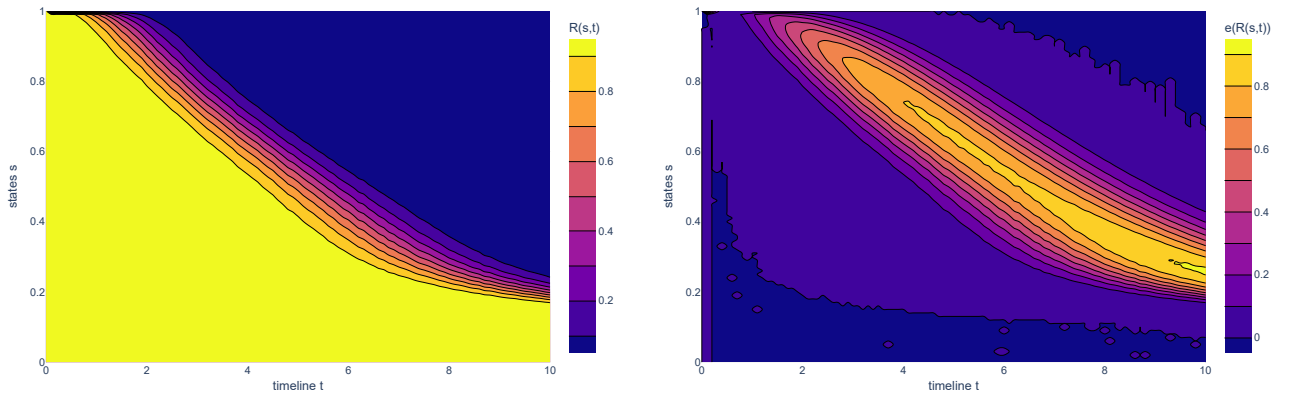

(a) Continuous-state survival function by means of DASC.

(b) Error between MCS estimate and DASC approximation.

Figure 21: 18-Component-Infrastructure-System: Contiunous-state survival functions computed by means of DASC and the corresponding error.

The continuous-state survival function obtained by means of the DASC is depicted in Figure 21a. The contour plot appears reasonable. As expected, the DASC achieves an approximation that in the worst case underestimates the true solution but never overestimates it. The theoretical findings can be verified when considering Figure 21b. The contour plot of the error between the MCS true solution estimate and the approximation is positive over the entire domain. Dark blue indicates an error magnitude of zero while dark purple represents magnitudes in the scale of machine precision.

The applied scheme already yields satisfying results taking into account that it is only a first-order scheme for at least diagonally state neutral structure functions. However, a higher-order implementation could significantly decrease the error in the remaining domain. In general, the proposed methodology is also applicable to diagonally state negative structure functions when adjusting the corresponding formula. For this example, it was ensured that the structure function is at least diagonally state neutral by accordingly specifying the exponential transformation function mapping component degradation to travel time. Figure 22 shows the true solution estimate of the continuous-state survival function obtained by means of MCS. The region of significant magnitudes of the error between the MCS and the DASC occurs as the underlying structure function is no longer diagonally state constant. As the structure function

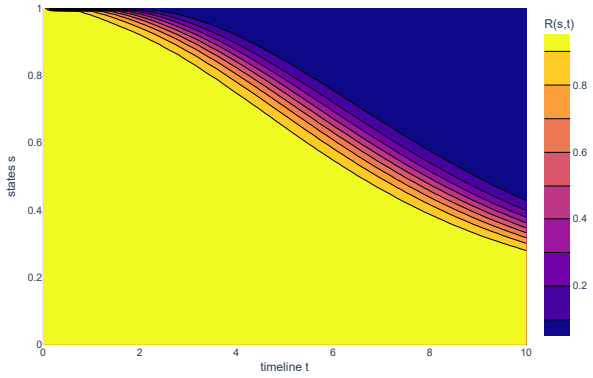

Figure 22: 18-Component-Infrastructure-System: MCS true solution estimate.

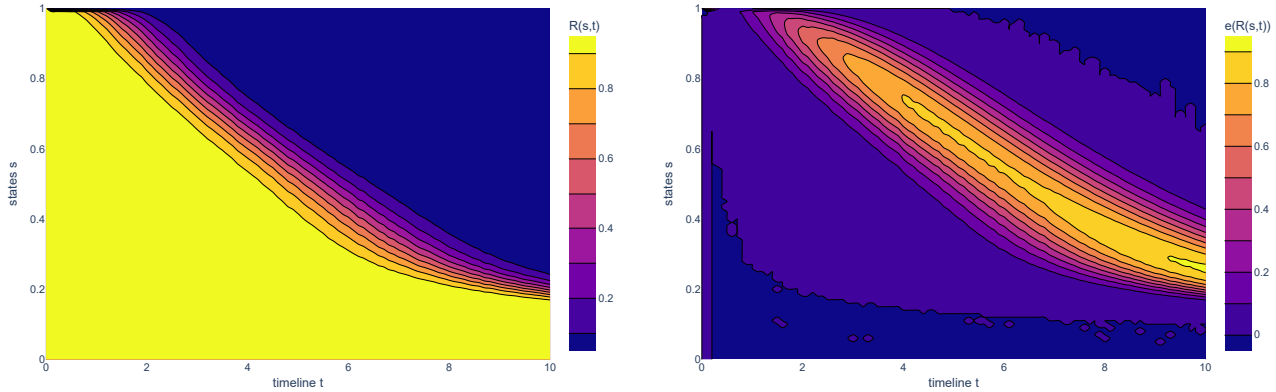

(a) Continuous-state survival function by means of DASCR.

(b) Error between MCS estimate and DASCR approximation.

Figure 23: 18-Component-Infrastructure-System: Continuous-state survival functions computed by means of DASCR with $r = 5$ and the corresponding error.

is still at least diagonally state neutral this is the only source for errors besides the natural variance of the stochastic degradation process.

The DASCR was applied to further increase the computational efficiency. In the following, the potential decrease of accuracy is studied. The proposed methodology still ensures pure underestimation of the true solution. For $r = 5$, compare Equation 21, the computation time already decreases significantly while the contour plots of the error appear similar, see Figure 23b.

For $r = 3$, the computation time can be further reduced as J decreases significantly. Thereby, it can be observed that the accuracy increases as all regions of error contour curves decrease in terms of their area, see Figure 24. The same observation can be made for $r = 2$: A tremendous reduction of computation time could be achieved as the DASCR further condenses the information in the DASC. By applying $r = 2$, J could be significantly decreased for all s along the diagonal of the state space and all l_s. In addition, it is noteworthy that the accuracy further increases, compare Figure 25 with Figure 24 and Figure 23.

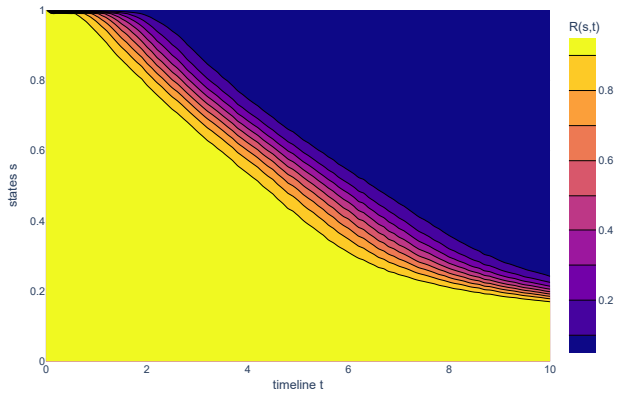

(a) Continuous-state survival function by means of DASCR.

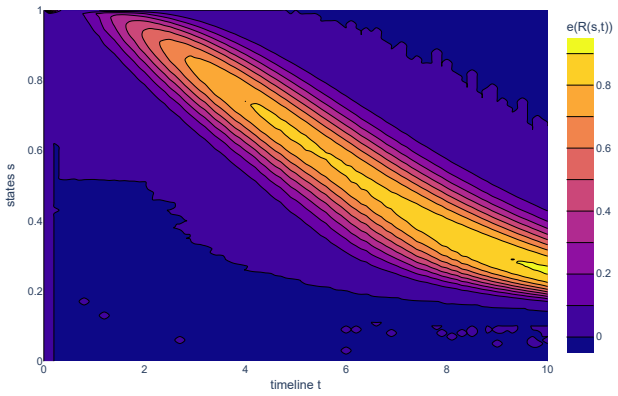

(b) Error between MCS estimate and DASCR approximation.

Figure 24: 18-Component-Infrastructure-System: Continuous-state survival functions computed by means of DASCR with $r = 3$ and the corresponding error.

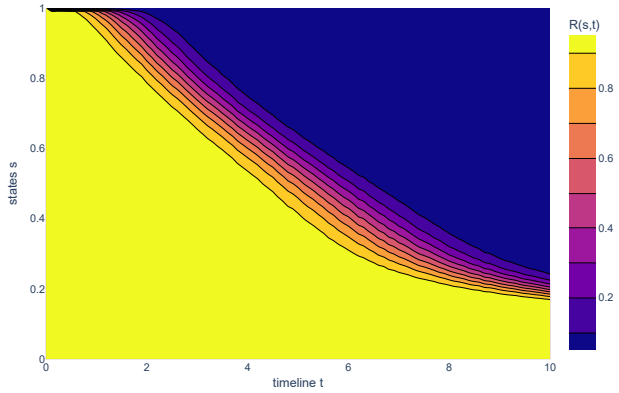

(a) Continuous-state survival function by means of DASCR.

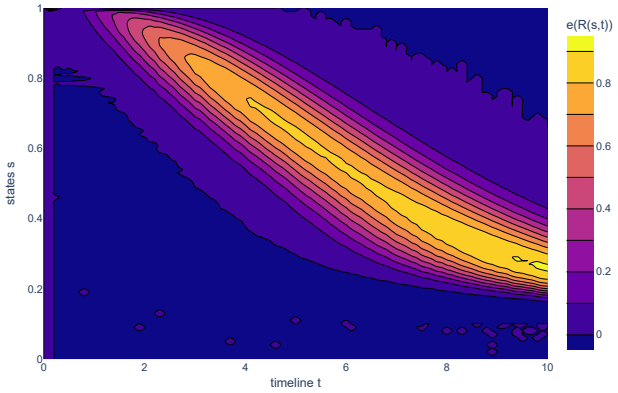

(b) Error between MCS estimate and DASCR approximation.

Figure 25: 18-Component-Infrastructure-System: Continuous-state survival functions computed by means of DASCR with $r = 2$ and the corresponding error.

5 Discussion

5.1 Case Studies

The case studies show that the DAS converges to the true solution of the continuous-state survival function for all MinMax-Systems regardless of their dimensionality. The global error vanishes for $N \to \infty$ as can be seen in the convergence studies. As the sample size N_{DAS} for the establishment of $R_x(s,t)$ is assigned to be large, the convergence of the MCS solutions to the DAS solution can be observed for all case studies conducted for the proof of concept. Besides the theoretical prove, these results underline the capability of the concept of DAS to achieve exact results for diagonally state constant systems. These findings verify in particular that the fundamental methodology introduced in Equation 14 can be utilized as explicit formula when considering a diagonally state at least neutral, diagonal state extreme and coherent structure function. Further, the results show that the computation time is independent of the sample

size when deploying the concept of DAS. For the DAS, the computation time in the online phase purely depends on the total number of components n and the number of considered components. Thereby, the DAS exhibits a linear relation between computation time and number of considered states, depending on the factor that is determined by n and correspondingly the binomial coefficient $\binom{n}{l_s}$. The observations coincide with the theory established in section 3. The formula Equation 14 is independent of the sample size N_{DAS} and clearly depending on the number of states that are considered and inserted as s. It can be observed that this basic approach becomes impractical for systems with $n >> 10$ combined with a number of considered states that is $>> 10$. For the first two case studies, the DAS still outperforms the MCS, although the evaluation of the corresponding structure function imposes minimal costs in the case of the MCS. This difference in computational effort becomes even more evident for more complex structure function.

The DASC was introduced and investigated as a naive solution to achieve increased computational efficiency also for larger systems that are characterized by an at least diagonally state constant and at least diagonally state neutral coherent structure function. The performance enhancement is achieved by condensing the DAS in terms of all possible permutations depending on l_s. In order to compute a DASC entry $\Psi(l_s, j) = (|C_j|, v_j)$, the number of occurrences of a value $\Phi(l_s, p)$ is determined and stored together with the value itself as a tuple. Thereby, the computational effort is reduced from a sum over $p = 1, 2, \ldots, \binom{n}{l_s}$ to a sum over $j = 1, 2, \ldots, J$, where J is the maximum number of different values for the DAS. The DASC shares the same convergence characteristics for diagonally state constant and extreme systems. Simultaneously, this approach exhibits significantly reduced numerical effort compared to its predecessor. The achieved reduction to J evaluations by means of information condensation is optimal with $J = 2$ for diagonally state extreme structure functions as the number of tuples $\Psi(l_s, j)$ for a given number of components working in state s or above l_s. This can be explicitly expressed as $v_j \in \{0, s\}$ and their corresponding occurences $|C_j(v_j)|$.

The application of the DASCR is not required for diagonally state extreme structure functions. In contrast, it is particularly useful when this criterion is not fulfilled. In the case of a diagonally state constant or higher order structure function, an iteration has to be performed in order to approximate the DAS for each combination of s, l_s and p. Values in the along the p-sum that are in the direct neighborhood in $[0, 1]$ are matched by means of a rounding procedure applied to $\Phi(l_s, p)$ and and $\Psi(l_s, j)$ is further condensed to $\Psi_r(l_s, j)$. Thereby, for a naive approach a trade-off has to be made in terms of computational cost and surrogate performance. Typically, it can be expected that $J_{r-1} \ll J_r$ but also that $|e_{r-1}(R(s,t))|_F \geq |e_r(R(s,t))|_F$, where $|e_r(R(s,t))|_F$ is the Frobenius norm of the error between the DASCR approximation and the theoretically available true solution. However, a sophisticated rounding procedure should check the lower and upper digits and determine the more favorable choice. Consequently, applying a sophisticated rounding procedure can improve the results obtained by DASC and DASCR with high r.

In the test of applicability for an arbitrary infrastructure system, the first-order DASC and DASCR5,3,2 perform well and underestimate the true solution of the continuous-state survival function as expected. Depending on the parameter $r \in \{5, 3, 2\}$ significant efficiency improvements can be achieved. The largest errors occur in the central region. The concepts of DAS become particularly useful for demanding structure functions. The evaluation of the weighted network efficiency is computationally more demanding than a composition of min- and max-operators. At the same time, highly demanding structure functions are neither diagonally state neutral or positive nor diagonally extreme or constant. Consequently, the proposed approaches can be applied in these cases when higher-order schemes are integrated or schemes for the estimation of the error are established. In contrast, conventional approaches could not address

such structure functions at all.

In its basic form, the DAS requires $\sum_s \sum_{l_s(n)} \sum_{p(l_s)}$ entries to be stored. The DASC already condenses the last sum that is the most critical for systems with a larger number of components up to a minimum of $J = 2$. Considering the storage requirement, the property of a structure function to be diagonally state invariant becomes important. However, note that for at least partly diagonally state invariant structure functions the entries of the $\Phi(l_s, p)$ and $\Psi(l_s, j)$ can be expressed in a linear relation for the range of s that is diagonally state invariant. The representation of the DAS and DASC by means of any type of function can enable to reduce the storage required among the first sum $\sum_s$, tremendously.

5.2 Comparison with Related Research

Subsequently, the developed concept of DAS is compared to approaches based on the concept of survival signature with regard to the properties of diagonal state sign, order, and variance and also based on the findings of the case studies. In [31], Eryilmaz & Tuncel introduced an explicit formula from a combinatorial perspective to compute a multi-state survival signature based on multiple path-wise binary-state structure functions to model the discrete multi-state perspective. The fundamental decomposition is based on the number of components in l_s. Thereby, the term path-wise corresponds to the terminology of a diagonally state extreme structure function. A classification in terms of the diagonal state sign is not reasonable in this case. The approach might consider diagonal state variance, as the structure functions can vary for each level. Theoretically, it is possible to define as many structure functions as states considered. In practice, however, this may prove infeasible when approaching a continuous view. However, these systems would still need to have some sort of path-wise measurability. The approach proposed in [34] by Qin & Coolen exhibits similar properties to those of the concept developed by Eryilmaz & Tuncel. The authors investigate discrete multi-state systems with multi-state components based on rule-based structure functions. In comparison with [31], Qin & Coolen developed a refined notation. The researchers based the combinatorial decomposition on the number of components working in state s. The computation of the multi-state survival function describing the probability of a system to be in state s or above is then performed in a post-processing step. In [33], Yi et al. proposed a fundamentally different approach on how to establish the discrete multi-state survival signature values. The authors adopt an probabilistic and conditional interpretation of the survival signature and further establish transformation relations [54].

Recent developments show that the survival signature finds increased attention in the field of stress-strength reliability. The works [55, 56] investigate approaches for statistical inference based on the concept of survival signature for multi-state system with multi-state components in this context. In [32], Liu et al. proposed an approach to compute $R(s)$ for discrete and multi-state systems with discrete and continuous multi-state stress-strength components. The authors applied their approach to diagonally state neutral, state invariant and state extreme systems. Thereby, a single vector is sufficient to represent the continuous-state survival signature of the diagonally state invariant systems with a single component type.

In contrast to the approaches presented above, the DAS was developed to evaluate the continuous-state survival function $R(s, t)$, introduced in subsection 3.1. Analogously, the concept of DAS and its variants can be utilized to compute $R(t)$ as well as $R(s)$. Recent literature in the context of survival signature addresses the computation of diagonally state extreme systems, i.e., path-wise measurable structure functions. In contrast, the methodology proposed in the current work enables surrogate modeling potentially for any kind of coherent structure function. Consequently, such structure functions might be diagonally state constant or of higher

order. In the case of structure functions that are of higher order, the current concept of DAS yields an approximation error. It appears practical to reduce this error by developing higher order schemes and more sophisticated rounding procedures for the concept of DAS. Some of the reviewed approaches take into account diagonally state variance by establishing one corresponding survival signature for each considered state or level. For diagonally state invariant structure functions the DASC(R) comprises $\sum_{l_s}^{n} \sum_{p(l_s)}^{J}$ elements. The conventional concepts of survival signature are only applicable to diagonally state extreme structure functions. Considering systems with a single component type and let them be diagonally state invariant for the ease of notation, conventional approaches require the storage of n values for the representation and the computation of the sum $\sum_{l_s}^{n}$ to evaluate $R(t)$ or $R(s)$ for a single t or s. In the same case, the DASC includes $\sum_{l_s}^{n} \sum_{p(l_s)}^{2}$ elements to be stored and evaluated. In summary, the DAS concept enables a broader range of application than similar and recently developed approaches, despite a slightly higher computational cost. The extent to which the range of applications can be broadened needs to be investigated in future work but the current findings appear promising.

5.3 Contextualization in Terms of Resilience

Three different approaches to determine $R(s,t)$ were outlined in section 3. Regardless of the approach utilized to establish $R(s,t)$, the continuous-state survival function inherently captures the probability of occurrence of disruptive events and their effect on the performance of the considered entity. Thus, $R(s,t)$ strongly relates to two properties of a system, reliability and robustness, shown in Figure 1, that govern its resilience when interpreted as in [17]. To show this theoretically, suppose that the performance deterioration over time being investigated empirically by exposing the entity to a certain environment in which potentially damaging effects or events occur in some frequency. Suppose the measurement only observes the state u_s at time t, where Δt between two time steps might be infinitesimal small. The occurrence of an event at t counts to the probability measure of the random variable to be less than s only if a deterioration in performance occurs as a consequence at the next time step under consideration. Thereby, the probability of the magnitude of the performance degradation of such a deteriorating event is intrinsically quantified as well. When established properly, both parts of information should also be captured when the continuous-state survival function is generated via stochastic processes modeling disruptive events either explicitly or implicitly. And similarly for the approach including a structure function, the disruptive events acting on components propagate their effects through the structure function $\phi(\boldsymbol{x})$ to the system state u_s and are captured by the continuous-state survival function. Eventually, despite not directly sampling a disruptive event from $R(s,t)$ but rather component performances, the occurrence of certain state sample is governed by the fundamental, measured or modeled disruptive events and the according response of the considered entity. Thereby, the structure function is critical for mitigating the effect of disruptive events acting on components. To conclude with regard to Figure 1, the continuous-state survival function quantifies not only if and when a performance deterioration occurs (reliability) but also its magnitude (robustness). The continuous-state survival function incorporates both notions simultaneously simply by representing the time-dependent probability distribution of each state of functionality.

In the context of the multidimensional and sub-structured resilience framework established in [25], the fact that $R(s,t)$ models both reliability and robustness can be exploited to enhance the stochastic simulation of subsystems as well as components during the evaluation of the resilience metric. For basic components, $R(s,t)$ can be established empirically or based on a stochastic process. Then, the generated $R(s,t)$ characterizing the stochastic degradation behavior are propagated from bottom level to top level of the sub-structured system. The

utilization of $R(s,t)$ allows for reduced computational effort in repeated evaluations of structure functions in subordinate levels during resilience optimization at $L \geq 1$ levels of subsystems. The concept of DAS enables a direct propagation of the $R(s,t)$ through each level by means of the explicit formulas provided in subsection 3.2. On the top-level, the overall structure function is evaluated by means of performance samples in order to quantify the resilience metric. The corresponding performances can be retrieved by sampling the state from the individual $R_i(s,t_c)$, where t_c denotes the currently considered time step. The DASC approach developed in the current work is immediately applicable to the case studies investigated in [25] after establishing a monotone sampling procedure based on $R(s,t)$. Future work addresses the detailed investigation concerning the integration of the continuous-state survival function as reliability and robustness representation into the resilience framework for sub-structured systems.

6 Conclusions & Outlook

In this work, the notion of the continuous-state survival function was presented and the concept of DAS was introduced as a corresponding surrogate modeling procedure. Thereby, the continuous-state survival function is defined as a time-dependent probability measure that characterizes the distribution of performance states of the considered system over time. This consideration gives engineers a new perspective when faced with the challenge of maintaining system performance in the face of disruptive events in a hostile environment. In light of the theoretical proof and the results in the case studies, the concept of DAS appears to be a solid foundation for more sophisticated surrogate modeling techniques. The relations to the phases characterized by reliability and robustness when quantifying system resilience were identified and discussed. The proposed methodology appears as an adequate approach to integrate a continuous-state consideration into a sub-structured resilience framework, as presented in [25].

In the course of this work, three different variants of the concept of DAS were established: At first, the fundamental statement Equation 14 was introduced to provide a comprehensive proof that DAS yields exact results for diagonal extremal and constant structure functions. For systems with a small number of components the DAS outperforms the MCS in terms of both computational time and accuracy. Secondly, the DASC Equation 20 was developed to overcome the limitations for larger systems. Moreover, DASCR was defined in Equation 21 to consider structure functions with a diagonal state order higher than constant. Thus, the current methodology extends the range of application of the separation property inherited by the concept of survival signature. It should be noted that the code can be further optimized, e.g., by integrating parallel computing. This leads to an additional increase in computational efficiency. In summary, the concepts of DAS developed in the current work show good results and open a rich and promising research topic.

The following items can be listed as critical developments concerning the concept of DAS as an autonomous surrogate modeling procedure but also in particular its integration into the resilience framework for complex and sub-structured systems [25].

- Integration into the resilience framework: The behavior of the DAS when integrated to the multidimensional and sub-structured resilience decision-making framework should be investigated in detail. The relationship between the endowment properties and the continuous-state survival function should also be explored.

- Broadening the range of application: Higher-order schemes should be addressed to reduce the approximation error for structure functions that are not diagonally state constant.

Further, the DAS formulas should be extended for diagonally state negative structure functions and multiple component types.

- Consideration of uncertainties: Extension of the DAS towards a consideration of uncertainties based on the proposed approach in [28] and integration into the multidimensional resilience decision-making framework for complex and sub-structured systems [25]. Approaches to reduce the storage requirements and to further condensate the developed formulas for enhanced efficiency during the online phase are of great interest.

7 Declarations

7.1 Authors' contributions

Made substantial contributions to conception and design of the work: Winnewisser NR, Salomon J, Broggi M;

Performed data analysis and interpretation: Winnewisser NR;

Provided administrative and technical support: Broggi M, Beer M

7.2 Availability of data and materials

Not applicable.

7.3 Financial support and sponsorship

This work was funded by the Deutsche Forschungsgemeinschaft (DFG, German Research Foundation) SPP 2388 501624329 and the "Reliability and Safety Engineering and Technology for large maritime engineering systems" (RESET) programme 730888.

7.4 Conflicts of interest

All authors declared that there are no conflicts of interest.

7.5 Ethical approval and consent to participate

Not applicable.

7.6 Consent for publication

Not applicable.

References

[1] G. P. Cimellaro, A. M. Reinhorn, and M. Bruneau, "Framework for analytical quantification of disaster resilience," *Engineering Structures*, vol. 32, no. 11, pp. 3639–3649, 2010.

[2] B. M. Ayyub, "Practical resilience metrics for planning, design, and decision making," *ASCE-ASME Journal of Risk and Uncertainty in Engineering Systems, Part A: Civil Engineering*, vol. 1, no. 3, p. 04015008, 2015.

[3] Y. Fang, N. Pedroni, and E. Zio, "Optimization of Cascade-Resilient Electrical Infrastructures and its Validation by Power Flow Modeling," *Risk Analysis*, vol. 35, no. 4, pp. 594–607, 2015.

[4] J. Bergström, R. Van Winsen, and E. Henriqson, "On the rationale of resilience in the domain of safety: A literature review," *Reliability Engineering and System Safety*, vol. 141, pp. 131–141, 2015.

[5] S. Hosseini, K. Barker, and J. E. Ramirez-Marquez, "A review of definitions and measures of system resilience," *Reliability Engineering & System Safety*, vol. 145, pp. 47–61, jan 2016.

[6] W. Sun, P. Bocchini, and B. D. Davison, "Resilience metrics and measurement methods for transportation infrastructure: the state of the art," *Sustainable and Resilient Infrastructure*, vol. 5, no. 3, pp. 168–199, 2020.

[7] I. Linkov and B. D. Trump, *The science and practice of resilience*. Springer, 2019.

[8] D. Henry and J. E. Ramirez-Marquez, "Generic metrics and quantitative approaches for system resilience as a function of time," *Reliability Engineering and System Safety*, vol. 99, pp. 114–122, 2012.

[9] T. Aven, "Improving the foundation and practice of reliability engineering," *Proceedings of the Institution of Mechanical Engineers, Part O: Journal of Risk and Reliability*, vol. 231, no. 3, pp. 295–305, 2017.

[10] B. M. Ayyub, "Systems resilience for multihazard environments: Definition, metrics, and valuation for decision making," *Risk analysis*, vol. 34, no. 2, pp. 340–355, 2014.

[11] R. Faturechi and E. Miller-Hooks, "Measuring the performance of transportation infrastructure systems in disasters: A comprehensive review," *Journal of infrastructure systems*, vol. 21, no. 1, p. 04014025, 2015.

[12] S. Galaitsi, J. M. Keisler, B. D. Trump, and I. Linkov, "The need to reconcile concepts that characterize systems facing threats," *Risk Analysis*, vol. 41, no. 1, pp. 3–15, 2021.

[13] K. B. Klaassen and J. C. Van Peppen, *System reliability*. VSSD, 2006.

[14] G. Punzo, A. Tewari, E. Butans, M. Vasile, A. Purvis, M. Mayfield, and L. Varga, "Engineering resilient complex systems: the necessary shift toward complexity science," *IEEE Systems Journal*, vol. 14, no. 3, pp. 3865–3874, 2020.

[15] S. Gilbert and B. M. Ayyub, "Models for the Economics of Resilience," *ASCE-ASME Journal of Risk and Uncertainty in Engineering Systems, Part A: Civil Engineering*, vol. 2, 2016.

[16] Y. Fang and G. Sansavini, "Optimizing power system investments and resilience against attacks," *Reliability Engineering and System Safety*, vol. 159, pp. 161–173, 2017.

[17] J. Salomon, M. Broggi, S. Kruse, S. Weber, and M. Beer, "Resilience decision-making for complex systems," *ASCE-ASME J Risk and Uncert in Engrg Sys Part B Mech Engrg*, vol. 6, no. 2, 2020.

[18] R. R. Singh, M. Bruneau, A. Stavridis, and K. Sett, "Resilience deficit index for quantification of resilience," *Resilient Cities and Structures*, vol. 1, no. 2, pp. 1–9, 2022.

[19] A. Alipour and B. Shafei, "An overarching framework to assess the life-time resilience of deteriorating transportation networks in seismic-prone regions," *Resilient Cities and Structures*, vol. 1, no. 2, pp. 87–96, 2022.

[20] S. Duan and B. M. Ayyub, "Assessment methods of network resilience for cyber-human-physical systems," *ASCE-ASME Journal of Risk and Uncertainty in Engineering Systems, Part A: Civil Engineering*, vol. 6, no. 1, p. 03119001, 2020.

[21] R. Emanuel and B. Ayyub, "Assessing resilience model responsiveness in the context of stakeholder preferences in decision support systems," *ASCE-ASME Journal of Risk and Uncertainty in Engineering Systems, Part A: Civil Engineering*, vol. 5, no. 2, p. 04019005, 2019.

[22] Y. Saadat, B. M. Ayyub, Y. Zhang, D. Zhang, and H. Huang, "Resilience-based strategies for topology enhancement and recovery of metrorail transit networks," *ASCE-ASME Journal of Risk and Uncertainty in Engineering Systems, Part A: Civil Engineering*, vol. 6, no. 2, p. 04020017, 2020.

[23] Y. Zhang, B. M. Ayyub, and J. F. Fung, "Projections of corrosion and deterioration of infrastructure in united states coasts under a changing climate," *Resilient Cities and Structures*, vol. 1, no. 1, pp. 98–109, 2022.

[24] L. Capacci, F. Biondini, and D. M. Frangopol, "Resilience of aging structures and infrastructure systems with emphasis on seismic resilience of bridges and road networks: Review," *Resilient Cities and Structures*, vol. 1, no. 2, pp. 23–41, 2022.

[25] J. Salomon, J. Behrensdorf, N. Winnewisser, M. Broggi, and M. Beer, "Multidimensional resilience decision-making for complex and substructured systems," *Resilient Cities and Structures*, vol. 1, no. 3, pp. 61–78, 2022.

[26] F. P. Coolen and T. Coolen-Maturi, "Generalizing the signature to systems with multiple types of components," in *Complex systems and dependability*, pp. 115–130, Springer, 2013.

[27] E. Patelli, G. Feng, F. P. Coolen, and T. Coolen-Maturi, "Simulation methods for system reliability using the survival signature," *Reliability Engineering & System Safety*, vol. 167, pp. 327–337, 2017.

[28] J. Salomon, N. Winnewisser, P. Wei, M. Broggi, and M. Beer, "Efficient reliability analysis of complex systems in consideration of imprecision," *Reliability Engineering & System Safety*, vol. 216, p. 107972, 2021.

[29] N. Jain, O. P. Yadav, A. P. S. Rathore, and R. Jain, "Reliability assessment framework for a multi-state multi-component system," *Journal of Industrial and Production Engineering*, vol. 34, no. 8, pp. 580–589, 2017.

[30] K. Yang and J. Xue, "Continuous state reliability analysis," in *Proceedings of 1996 Annual Reliability and Maintainability Symposium*, pp. 251–257, IEEE, 1996.

[31] S. Eryilmaz and A. Tuncel, "Generalizing the survival signature to unrepairable homogeneous multi-state systems," *Naval Research Logistics (NRL)*, vol. 63, no. 8, pp. 593–599, 2016.

[32] Y. Liu, Y. Shi, X. Bai, and B. Liu, "Stress–strength reliability analysis of multi-state system based on generalized survival signature," *Journal of Computational and Applied Mathematics*, vol. 342, pp. 274–291, 2018.

[33] H. Yi, L. Cui, and N. Balakrishnan, "Computation of survival signatures for multi-state consecutive-k systems," *Reliability Engineering & System Safety*, vol. 208, p. 107429, 2021.

[34] J. Qin and F. P. Coolen, "Survival signature for reliability evaluation of a multi-state system with multi-state components," *Reliability Engineering & System Safety*, vol. 218, p. 108129, 2022.

[35] L. Skyttner, "General systems theory: origin and hallmarks," *Kybernetes*, 1996.

[36] J. C. Hudson and K. C. Kapur, "Reliability bounds for multistate systems with multistate components," *Operations Research*, vol. 33, no. 1, pp. 153–160, 1985.

[37] M. L. Gámiz and M. M. Miranda, "Regression analysis of the structure function for reliability evaluation of continuous-state system," *Reliability Engineering & System Safety*, vol. 95, no. 2, pp. 134–142, 2010.

[38] J. C. Hudson and K. C. Kapur, "Reliability analysis for multistate systems with multistate components," *AIIE Transactions*, vol. 15, no. 2, pp. 127–135, 1983.

[39] F. P. Coolen and T. Coolen-Maturi, "The structure function for system reliability as predictive (imprecise) probability," *Reliability Engineering & System Safety*, vol. 154, pp. 180–187, 2016.

[40] G. Feng, E. Patelli, M. Beer, and F. P. Coolen, "Imprecise system reliability and component importance based on survival signature," *Reliability Engineering & System Safety*, vol. 150, pp. 116–125, 2016.

[41] F. J. Samaniego, *System signatures and their applications in engineering reliability*, vol. 110. Springer Science & Business Media, 2007.

[42] C. E. Ebeling, *An introduction to reliability and maintainability engineering*. Waveland Press, 2019.

[43] K. Beata, K. Dariusz, and M. Dariusz, "Survival function in the analysis of the factors influencing the reliability of water wells operation," *Water Resources Management*, vol. 33, pp. 4909–4921, 2019.

[44] J. Zhang, M. Zhao, H. Liu, and X. Xu, "Networked characteristics of the urban rail transit networks," *Physica A: Statistical Mechanics and its Applications*, vol. 392, no. 6, pp. 1538–1546, 2013.

[45] V. Latora and M. Marchiori, "Efficient behavior of small-world networks," *Physical Review Letters*, vol. 87, no. 19, pp. 198701–1–198701–4, 2001.

[46] S. E. Dreyfus, "An Appraisal of Some Shortest-Path Algorithms," *Operations Research*, vol. 17, no. 3, pp. 395–412, 1969.

[47] F. B. Zhan and C. E. Noon, "Shortest Path Algorithms: An Evaluation Using Real Road Networks," *Transportation Science*, vol. 32, pp. 65–73, 1998.

[48] V. Latora and M. Marchiori, "Economic small-world behavior in weighted networks," *The European Physical Journal B-Condensed Matter and Complex Systems*, vol. 32, no. 2, pp. 249–263, 2003.

[49] X. Wang and D. Xu, "An inverse gaussian process model for degradation data," *Technometrics*, vol. 52, no. 2, pp. 188–197, 2010.

[50] Z.-S. Ye and N. Chen, "The inverse gaussian process as a degradation model," *Technometrics*, vol. 56, no. 3, pp. 302–311, 2014.

[51] W. Peng, Y.-F. Li, Y.-J. Yang, J. Mi, and H.-Z. Huang, "Bayesian degradation analysis with inverse gaussian process models under time-varying degradation rates," *IEEE Transactions on Reliability*, vol. 66, no. 1, pp. 84–96, 2017.

[52] L. Trippa, P. Müller, and W. Johnson, "The multivariate beta process and an extension of the polya tree model," *Biometrika*, vol. 98, no. 1, pp. 17–34, 2011.

[53] F. Daum and J. Huang, "Curse of dimensionality and particle filters," in *2003 IEEE aerospace conference proceedings (Cat. No. 03TH8652)*, vol. 4, pp. 4_1979–4_1993, IEEE, 2003.

[54] H. Yi, N. Balakrishnan, and X. Li, "Multi-state joint survival signature for multi-state systems with shared multi-state components," *Methodology and Computing in Applied Probability*, vol. 25, no. 1, p. 44, 2023.

[55] X. Bai, X. Li, N. Balakrishnan, and M. He, "Statistical inference for dependent stress–strength reliability of multi-state system using generalized survival signature," *Journal of Computational and Applied Mathematics*, vol. 390, p. 113316, 2021.

[56] X. Bai, J. Zhang, M. He, and N. Balakrishnan, "Inference for stress–strength reliability of multi-state system with dependent stresses and strengths using improved generalized survival signature," *Journal of Computational and Applied Mathematics*, vol. 420, p. 114809, 2023.